FOI
SWEDISH DEFENCE
RESEARCH AGENCY

FOI-R--0441--SE
March 2002
ISSN 1650-1942
Scientific Report

Roman Starikov

Mechanically fastened joints: Critical testing of single overlap joints

Aeronautics Division, FFA
SE-172 90 Stockholm
Sweden

SWEDISH DEFENCE RESEARCH AGENCY
Aeronautics Division, FFA
172 90 Stockholm
Sweden

FOI-R--0441--SE
March 2002
ISSN 1650-1942
Scientific Report

Roman Starikov

Mechanically fastened joints: Critical testing of single overlap joints

Issuing organization	Report number, ISRN	Report type
FOI – Swedish Defence Research Agency Defence Analysis SE-172 90 Stockholm	FOI-R--0441--SE	Scientific report
	Research area code 7. Vehicles	
	Month year March 2002	**Project no.** E824629
	Customers code 5. Contracted Research	
	Sub area code 73 Aeronautical Research	

Author/s (editor/s)	Project manager
Roman Starikov	Roman Starikov
	Approved by Anders Blom Head, Structures Department
	Scientifically and technically responsible

Report title

Mechanically fastened joints: Critical testing of single overlap joints

Abstract (not more than 200 words)

The structural integrity of critical aircraft metal structures, which include bolted joints, has to be validated according to the certification requirements. The objective of the present work is to improve the understanding of the static and fatigue behaviour of single overlap aluminium bolted joints. Three joints were loaded in static with three different pre-tensions in the bolts. Strain gauges were used to measure strain distributions between the bolt rows and calculate secondary bending at different joint locations. Two instrumented bolts were employed to measure their axial and shear response during loading. An optical measurement method, Digital Speckle Photography (DSP), was applied to measure bolt movement at different fastener locations. After the static programme, the same joints were tested in spectrum until a different number of blocks. The same measurement procedure was carried during spectrum testing. The load transfer between the bolt rows was calculated using the measured strain distribution. The achieved results were then compared with those ones obtained from measurements done on the instrumented bolts. The overall test results indicated that the friction forces between the joint parts affected significantly the load-transfer distribution in the joints. The initial level of pre-tension in the bolts was a very important issue influencing the load transfer as well as secondary bending. The obtained experimental results could be implemented in finite element modeling of mechanically fastened joints.

Keywords

Bolted joints; Static; Spectrum loading; Instrumented bolts; Strain measurement; Load transfer; Bolt movement

Further bibliographic information	Language English
ISSN 1650-1942	**Pages** 58 + doc. p.
	Price acc. to pricelist
	Security classification

Utgivare	Rapportnummer, ISRN	Klassificering
Totalförsvarets Forskningsinstitut - FOI Flygteknik, FFA 172 90 Stockholm	FOI-R--0441--SE	Vetenskaplig rapport
	Forskningsområde 7. Bemannade och obemannade farkoster	
	Månad, år March 2002	**Projektnummer** E824629
	Verksamhetsgren 5. Uppdragsfinansierad verksamhet	
	Delområde 73 Flygteknisk forskning	

Författare/redaktör	Projektledare
Roman Starikov	Roman Starikov
	Godkänd av Anders Blom Institutionschef
	Tekniskt och/eller vetenskapligt ansvarig

Rapportens titel (i översättning)

Mekaniska förband: Kritisk provning av enskäriga överlappsskarvar

Sammanfattning (högst 200 ord)

Strukturintegriteten för kritisk metallstruktur i flygplan som innehåller bultade förband måste valideras i enlighet med certifieringsbestämmelserna. Syftet med föreliggande arbete är att förbättra förståelsen för såväl det statiska beteendet som utmattnings-beteendet hos enkla bultade överlappsförband i aluminium. Tre förband med tre olika bultförspänningar belastades statiskt. Töjningsgivare användes för att mäta töjnings-fördelningar mellan bultraderna och för att beräkna sekundärböjningen i vissa utvalda punkter i förbanden. Två instrumenterade bultar användes för att mäta deras axial- och skjuvresponser i samband med belastning av förbanden. En optisk mätmetod, "Digital Speckel Fotografering (DSP)" användes för att registrera rörelsen hos bultarna i fäst-elementhålen. Efter det statiska mätprogrammet spektrumutmattades förbanden med olika antal lastsekvensblock. Samma mätprogram som i den statiska delen tillämpades även under spektrumutmattningen. Lastöverföringen mellan bultraderna beräknades utifrån den uppmätta töjningsfördelningen. De erhållna resultaten jämfördes mot de som erhölls från de instrumenterade bultarna. Det övergripande resultatet indikerar att friktionen mellan plåtarna i överlappsförbandet på ett signifikant sätt påverkar last-överföringsfördelningen i förbandet. Den ursprungliga nivån hos klämkraften i bultarna var mycket betydelsefull både avseende lastöverföring och sekundärböjning. De erhållna experimentella resultaten kan utnyttjas vid finit element modellering av mekaniska förband.

Nyckelord

Skruvförband, Statisk belastning, Spektrum belastning, Instrumenterade skruvar, Töjningsmätning, Lastöverföring, Skruvrörelser

Övriga bibliografiska uppgifter	Språk Engelska
ISSN 1650-1942	**Antal sidor:** 58 + doc s.
Distribution enligt missiv	**Pris: Enligt prislista** **Sekretess**

Abstract

The structural integrity of critical aircraft metal structures, which include bolted joints, has to be validated according to the certification requirements. The objective of the present work is to improve the understanding of the static and fatigue behaviour of single overlap aluminium bolted joints. Three joints were loaded in static with three different pre-tensions in the bolts. Strain gauges were used to measure strain distributions between the bolt rows and calculate secondary bending at different joint locations. Two instrumented bolts were employed to measure their axial and shear response during loading. An optical measurement method, Digital Speckle Photography (DSP), was applied to measure bolt movement at different fastener locations. After the static programme, the same joints were tested in spectrum until a different number of blocks. The same measurement procedure was carried during spectrum testing. The load transfer between the bolt rows was calculated using the measured strain distribution. The achieved results were then compared with those ones obtained from measurements done on the instrumented bolts. The overall test results indicated that the friction forces between the joint parts affected significantly the load-transfer distribution in the joints. The initial level of pre-tension in the bolts was a very important issue influencing the load transfer as well as secondary bending. The obtained experimental results could be implemented in finite element modeling of mechanically fastened joints.

Keywords: Bolted joints; Static; Spectrum loading; Instrumented bolts; Strain measurement; Load transfer; Bolt movement

Contents

1 Introduction

Mechanically fastened joints provide the primary means for transferring loads among components in the construction of aircraft structures. However, the presence of holes is associated with high stress concentrations, which may lead to crack initiation from the hole boundary followed by catastrophic failure of the joint structure. Therefore, the mechanical performance of fastened joints has been the subject of numerous analytical and experimental approaches for many years. There have been pointed out several parameters that have to be taken into account when the mechanical behaviour of aluminium bolted joints is analysed.

1.1 Fretting wear and fatigue in bolted joints

Aluminium bolted joints loaded in fatigue suffer from fretting damage in the faying surfaces of the joined plates. According to the definition given by Szolwinski and Farris, fretting is a contact damage process arising from surface microslip associated with small-scale oscillatory motion of clamped structural members [1]. Fretting combines fretting wear, corrosive, and fretting fatigue. Moreover, fretting fatigue is recognized as a mechanism of the formation of cracks in structural joined members, which often leads to multi-site damage in mechanically fastened joints in aging aircraft. There have been reported three stages of the damage formation due to fretting of the faying surfaces [1]. During the first stage the thin oxide layer is removed from the plate surface due to mechanical wear processes. At the same time, the origin metal of the contact surfaces starts to adhere. This process results in the initial formation of wear debris between the contact surfaces.

The next stage is characterized by the appearance of near-surface plastic deformation in the contact areas, additional wear and the potential formation of new oxide. The first event can result in the nucleation of grain-sized microcracks. With further loading, these microcracks may either be worn away or propagate below the material surface and merge with other cracks.

The last stage in the three-stage damage mechanism is driven by the transition from fretting wear to fretting fatigue, which is evidenced by the propagation of such a crack or several of them into the bulk material. At this stage, the influence of the contact forces becomes less dominant since the crack growth is governed by the global stresses [1].

The role of fretting in the degradation of aircraft structures has been studied extensively last years on both in-service aircraft and laboratory specimens. There are several typical sites from which fretting fatigue damage may start to propagate. Three failure origins were observed in an experimental work on the fatigue durability of aluminium bolted joints [2]. Fatigue cracks induced by fretting between the bolt shank and the plates were observed in the hole surface at multiple sites. The next site was asso-

ciated with the surface close to bolt holes, which were cold-expanded prior to testing. In this case fretting of the out-of-plane protrusions on the faying surfaces was the cause of the damage formation and propagation. The last failure origin was located on a certain distance from the holes. In some cases fretting was not the cause of the nucleation of surface cracks since they originated from surface inclusions in grains [2]. Similar fatigue crack initiation sites were reported in the obtained results of a fractographic observation of aluminium joints bolted by different fastener systems [3]. Four types of fatigue crack initiation were divided depending on their location relatively to the bolt hole, i.e. the net section or ahead of the bolt, and the corresponding mechanism inducing the damage nucleation, i.e. high stress concentration at the bolt hole and fretting in the faying surfaces. In both experimental works the appearance of the fracture origins varied with the assembly conditions. Moreover, as was pointed out in [3], the fatigue durability strongly depended on the site of fatigue crack initiation.

1.2 Bolt pre-tension

An initial amount of clamping force in bolts has a significant influence on the joint response to applied static and fatigue loading [4]-[6]. It is recognized that high initial pre-tensions in the bolts result in a larger part of the applied load being transferred by the friction forces between the joint plates. Therefore, such joints would perform better resistance to either static or fatigue loading. As has already been mentioned, the assembly conditions, which include the initial pre-tension in the bolt and different fastener configurations, affect the site of the fatigue crack formation [3]. On the other hand, since high clamping forces result in high friction between the joint parts, this leads to fretting fatigue becoming more dominant in the fatigue damage development in the joint. Therefore, an optimum amount of the initial pre-tension has to be chosen depending on the assembly condition and joint configuration. As was reported, due to the Poisson's effect of loaded plates, there was a reduction in the plate thickness, which, in turn, could reduce the pre-tension in the bolt, and thereby caused a reduction in the clamping force experienced by the joined plates [6]. However, this was not proved experimentally.

1.3 Secondary bending

Mechanically fastened joints may be implemented either with a single overlap or double lap configuration. The first configuration is recognized as prone to secondary bending during loading. This event causes bending deflection of the bolt and joint plates which usually results in non-uniform stress distribution through the thickness of the joined plates. As paper [2] cites, after strain gauging 150 aircraft structural details, 86% exhibited secondary bending although they are quite often supported by stiffners, spars,

or wing boxes. In order to eliminate the effect of secondary bending and buckling out-of-plane deflection, an anti-buckling lateral support is used. As the obtained results of a numerical calculation approach present, compression loads and skin buckling of mechanically fastened fuselage panels had a significant effect on the circumferential stress in the skin and fastener loads, which would influence damage initiation [13]. The same parameters had a comparable effect on stress intensity factors for the cases with modeled cracks. This influenced the damage propagation rates and the residual strength of the panel. As an experimental work on the fatigue resistance of non-bending and bending high-load-transfer joints presented, secondary bending could decrease the fatigue durability of the tested joints [2].

In experimental approaches the effect of secondary bending can be studying using strain gauge technique [7], [8], [14]. Since this method requires strain gauges to be glued on both sides of the inspected plate, it gives rather limited information about secondary bending along all length of the joint. Therefore, the application of special optical or thermal emissions methods would be more effective in analysing the influence of secondary bending [8], [11]. Moreover, from the literature review it seems that there is no exact definition of how to determine secondary bending since it could be different from one measured in the joint-overlap area and that obtained in non-overlap region for the same joint plate.

1.4 Load transfer

Since the main objective of mechanically fastened joints is to transfer applied load from one part to another via fasteners, the load distribution between the joint members is a very important issue. This subject can be studied using strain gauges and the following integration of the measured strain distribution between bolt rows [3], [8], [14]-[16]. According to several experimental works with the application of strain gauge measurements, bolt rows carry different amounts of applied load [15], [16]. The same result was achieved using a thermo-elastic stress analyzer to measure the stress distribution between different fasteners in riveted joints [4]. However, the strain gauge method does not represent the influence of friction on the load transfer since the friction forces are considered to be included into the measurement results. Therefore, the application of special bolts, instrumented with specially oriented strain gauges, should give a more accurate analysis of the load transfer between the joined plates and the friction [8]. This measurement method has been successfully used in static and spectrum testing to observe the load-transfer distribution in bolted joints with a different configuration [9]. It was reported that the load transferred by the friction forces between the joint plates increased substantially during fatigue loading. This was due to an increase in the coefficient of friction of the plates as a result of fretting wear between them.

1.5 Objectives of present study

The main objectives of this work were to collect experimental data on the behaviour of aluminium bolted joints subjected to static and spectrum loading. The influence of different fastener systems and clamping forces on the joint performance would be studied. Strain gauge measurements would be carried out in order to measure secondary bending and calculate the load transfer between bolt rows. The achieved results would be compared with those ones obtained from measurement in instrumented bolts. An optical measurement method would be employed in order to measure bolt movement on different fasteners. The overall experimental results gained from the experimental work could be used in future finite element modeling of mechanically fastened joints.

2 Testing procedure

2.1 Specimen configuration

In total, three joints were prepared for static and spectrum tests. Each specimen was assembled from two aluminium alloy AA7475-T761 plates using four countersunk Hi-Lok fasteners to implement a single overlap joint configuration. The geometry of the plates and the joint configuration are shown in Fig. 1.

Figure 1. Specimen geometry and configuration. Dimensions in [mm].

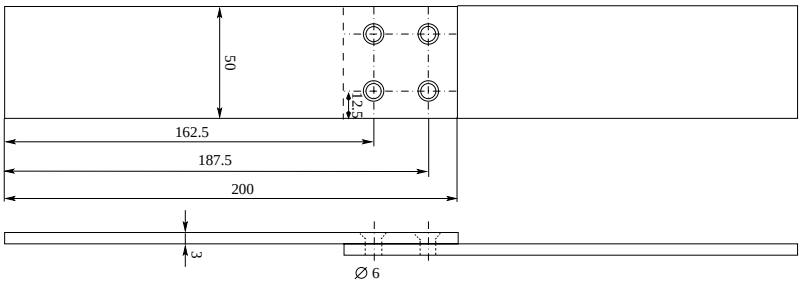

The fasteners were manufactured from 6Al-4V titanium alloy material with a shank diameter of 6 mm.

2.2 Specimen instrumentation

2.2.1 Strain gauges

In order to analyse load transfer between the bolt rows and secondary bending during quasi-static and spectrum loading, the plate with countersunk holes was equipped with strain gauges as shown in Fig. 2.

Figure 2. Location of strain gauges. Dimensions in [mm].

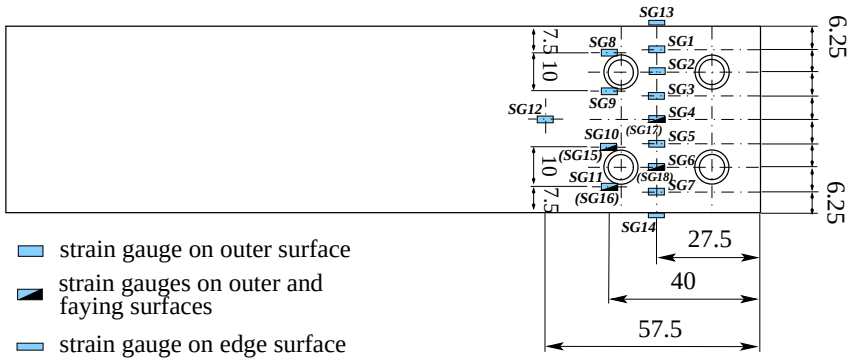

Technical data of the strain gauges are summarized in Table 1.

Table 1. Specification of strain gauges.

Type:	HBM 3/120LY13
Gauge resistance:	120 Ohms
Gauge factor:	2.04
Dimensions:	1.4 × 3.0 mm

To accommodate the wiring from the strain gauges located on the faying surface, 0.6 mm deep slots were milled in the joint part with ordinary holes.

2.2.2 Instrumented bolts

To be able to analyse bolt axial and shear forces, two fasteners were instrumented with strain gauges (instrumentation numbers: CSK 1 and CSK 2). Each bolt was equipped with two rosette strain gauges located in such a way to measure shear strain in the plane of the faying surface of the specimen. Figure 3 shows an instrumented bolt with an external rosette strain gauge. Another strain gauge of the same type was glued on the opposite side of the bolt shank as well.

Figure 3. Instrumented bolt with rosette strain gauges.

A special external bridge was used in order to collect data on the strain gauges. The rosette gauges were connected in such a way to be able to measure either axial or shear deformation during loading by setting up the external bridge. During loading measurement data from both rosette strain gauges were recorded as one balanced signal.

2.3 Optical measurement

An optical measurement method, Digital Speckle Photography (DSP), was applied to measure bolt movement on different fasteners (see Fig. 4). A metal plate with a pin was glued to the head of two bolts as shown in Fig. 4(b).

Figure 4. Application of Digital Speckle Photography. Dimensions in [mm].

(a)

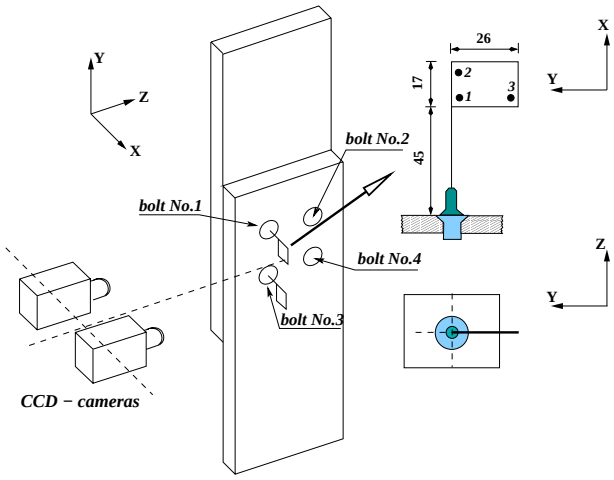

(b)

A spray paint was applied onto the plate surface in order to create a random pattern [11]. Before loading the initial position of the plates was recorded using two CCD-cameras (CCD - Charged Coupled Devise). Through this it was possible to carry out displacement measurements in the three, *X-Y-Z*, directions. During loading the plate displacement was recorded after a certain increment in the applied load. Further, three points were chosen on the plate surface (see the flag with marked points *1, 2, 3* drawn in Fig. 4(b)). Using the data analyse tool the displacement of the points was represented and used to observe bolt bending and bolt rotation.

Bolt movement may consist of several events. So, that bolt movement measured in the *X-Y* plane, is further referred as bolt bending (see Fig. 4(b)); whereas bolt movement, which was observed in the *Y-Z* plane, corresponds to bolt rotation.

2.4 Loading configuration

2.4.1 Calibration of instrumented bolts

The instrumented bolts were calibrated in tension and shear. A special load fixture, which was developed and used frequently for the calibration procedure of instrumented bolts at FFA [9], being subjected to compressive load, introduces tensile load in the instrumented bolt.

Two plates of the same thickness and aluminium material as the joint plates were used for shear calibration in the form of a single bolt joint. The plates were fastened with a finger torque applied to the instrumented bolt.

2.4.2 Static testing

Each specimen was quasi-statically loaded several times with different pre-stresses in the bolts for each loading series. Table 2 shows three levels of the initial pre-torque applied to the fasteners.

Table 2. Specified pre-torque levels and installation methods of fasteners for static experiments.

Pre-torque level	Fastener installation
Finger tight	Ordinary nuts and washers
Pre-tension of 3.5 kN	Ordinary nuts and washers
Maximum torque	Hi-Lok nuts and washers

During the calibration of the instrumented bolts, a relationship between the applied tensile load and axial deformation was obtained. Then, during the joint assembly the instrumented bolts were tightened until the specified axial pre-load had been achieved.

2.4.3 Spectrum testing

After the static tests had been performed, the specimens were subjected to spectrum loading. The standard load spectrum FALSTAFF (Fighter Aircraft Loading STAndard For Fatigue evaluation) was used to test the bolted joints in spectrum. A gross section stress level of 150 MPa was used for the testing. There were three different load sequence lengths, SHORT, MEDIUM, and LONG to which the specimens were subjected (see Table 3.)

Table 3. Spectrum test programme.

Specimen	Spectrum test	Number of FALSTAFF sequences
1	SHORT	20
2	MEDIUM	60
3	LONG	Until visible crack

The SHORT life test corresponds to a single life for a fighter aircraft, i.e. 4000 flights, which is equivalent to 20 FALSTAFF sequences. The MEDIUM life test is based on the design life according to the standard

damage tolerance approach. The design life corresponds to two times the aircraft service life. Thus, the MEDIUM life was chosen as 3/4 of the design life, which corresponds to 60 FALSTAFF sequences. In the case of the LONG life test, the specimen was supposed to be loaded until a visible crack would be observed.

Since the spectrum testing involved compressive loads, an anti-buckling fixture was used in order to prevent global buckling of the specimen. Figure 5 shows the geometry and configuration of the anti-buckling support.

Figure 5. Anti-buckling support. Dimensions in [mm].

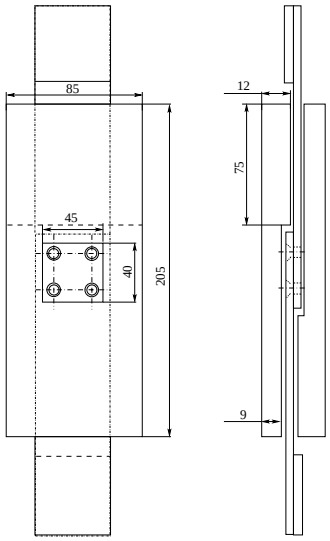

To reduce the influence of the friction forces between the specimen and the lateral support, they were interleaved with Teflon sheets of a 2 mm thickness. The specimen bolts were assembled with Hi-Lok nuts. During their installation, the axial strain in the instrumented bolts was measured. Data acquisition from the instrumented bolts, the strain gauges, and the optical system was taken after a certain number of FALSTAFF sequences specified in Table 4 for each specimen in particular.

Table 4. Matrix of data acquisition on instrumented bolts.

Life test length	Number of FALSTAFF sequences	Measurement in bolts
LONG, MEDIUM, SHORT	1	Shear + axial
LONG, MEDIUM, SHORT	2	Shear
LONG, MEDIUM, SHORT	5	Shear
LONG, MEDIUM, SHORT	10	Shear
LONG, MEDIUM, SHORT	20	Shear + axial*
LONG, MEDIUM	60	Shear + axial**
LONG	95	Shear
LONG	120	Shear + axial

* Axial measurement only on SHORT life specimen
** Axial measurement only on MEDIUM life specimen

The sequence of data acquisition is illustrated in Fig. 6.

Figure 6. Sequence of data acquisition.

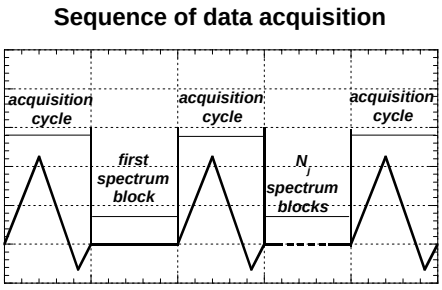

The maximum and minimum load levels in a data acquisition cycle correspond to the maximum and minimum load peaks from one FALSTAFF spectrum block, i.e. 150 and -39 MPa of applied stress.

3 Experimental results

3.1 Bolt calibration

Each instrumented bolt was calibrated in tension and shear. The obtained calibration results are presented in Fig. 7, where bolts No. 1 and No.2 correspond to instrumented bolts CSK1 and CSK2, respectively.

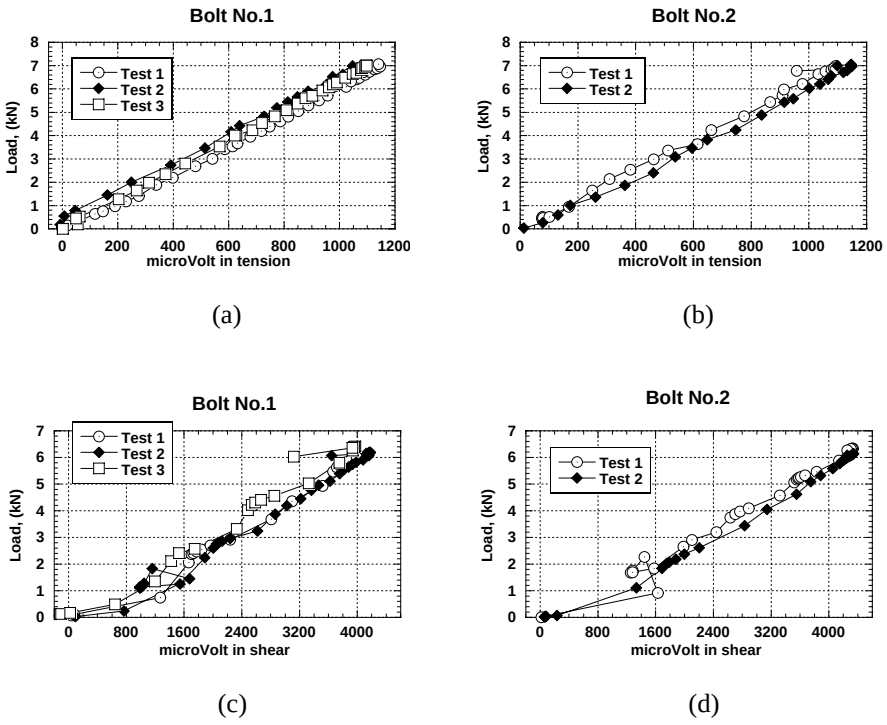

Figure 7. Results of calibra tests: (a) and (b) calibratio tension; (c) and (d) calibratio shear.

In general, both instrumented bolts performed similar calibration characteristics since they showed almost the same value of the measured tensile and shear deformations during loading. As can be seen in Fig. 7(a) and (b), the tensile curves show a linear behaviour during static loading. The loading curves for the shear calibration tests show some nonlinearity at the very beginning of loading. At this stage the instrumented bolts were settling themselves in the bolt hole under loading. When the applied load was further increased, they started to transfer load and the strain gauges measured a linear increase in the bolt deformation until the maximum load level was reached.

Along with the calibration of the instrumented bolts in tension and shear, they were subjected to a tightening torque versus axial deformation calibration. Through this the required level of clamping force in non-instrumented bolts was possible to achieve. Each instrumented bolt was tightened with a different torque moment using a torque wrench. During this procedure the axial deformation of the bolts was observed. The application of each torque moment was repeated five times. Figure 8 shows the

applied torque versus axial deformation lines for each instrumented bolt. Marks in the plot are an average value of the axial strain measured for the five repetitions.

Figure 8. Applied torque vs axial strain calibration results.

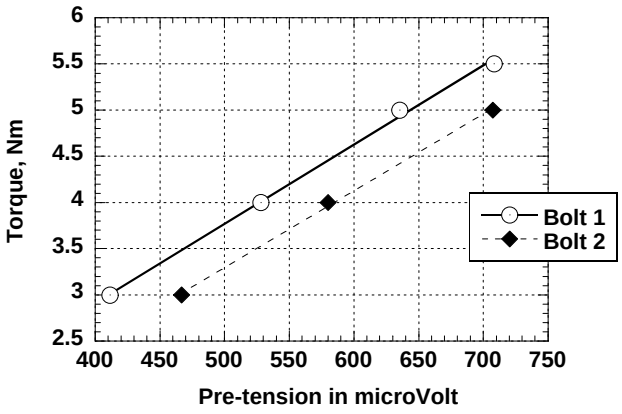

Although the lines show a linear relationship between the axial deformation and the applied torque moments, there is a difference in the bolt responses on the tightening torque, which might be due to the influence of friction between the bolt and the washer during the tightening procedure.

The obtained linear relationship between the axial deformation and applied torque moments was used together with the axial calibration results, see Fig. 7(a) and (b), to estimate a torque moment to which the ordinary bolts should be tightened in order to achieve their initial 3.5 kN pre-tension.

3.2 Static tests

3.2.1 Measurement in instrumented bolts

Figure 9 shows the measured results of the axial strain for the first joint tested in static with the three different initial pre-torque levels in the bolts. For each pre-torque level loading was repeated two times. The arrows indicate the direction of the curves. In the plots, the bolt numbers reflect the location of these bolts in the specimen, see Fig. 4(b), i.e. bolts Nos. 2 and 4 in Fig. 9 correspond to bolts Nos. 1 and 2 in Figs. 7 and 8, respectively. The axial measurement results for the other two specimens are presented in Fig. 10(a) and (b). Figure 10(c) and (d) shows the obtained results of the axial measurement done on the third specimen tested with the lateral support.

Figure 9. Specimen No.1: axial measurement in instrumented bolts.

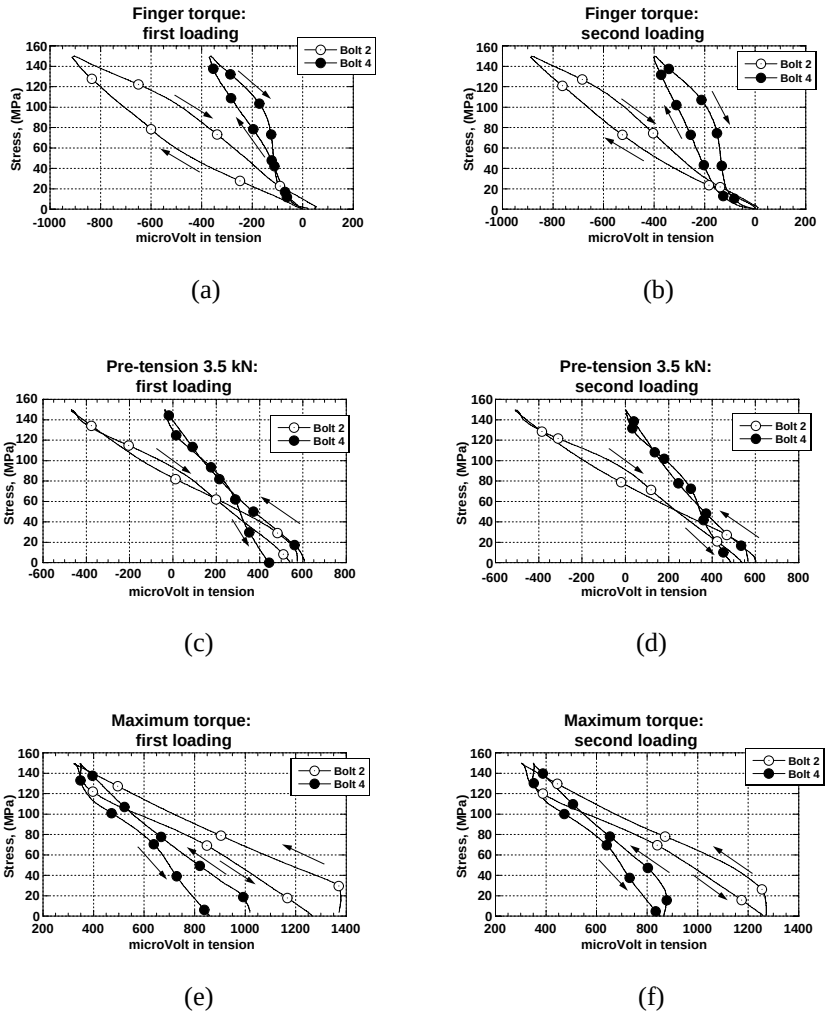

Figure 10. Specimens No.2 and 3: axial measurement in instrumented bolts.

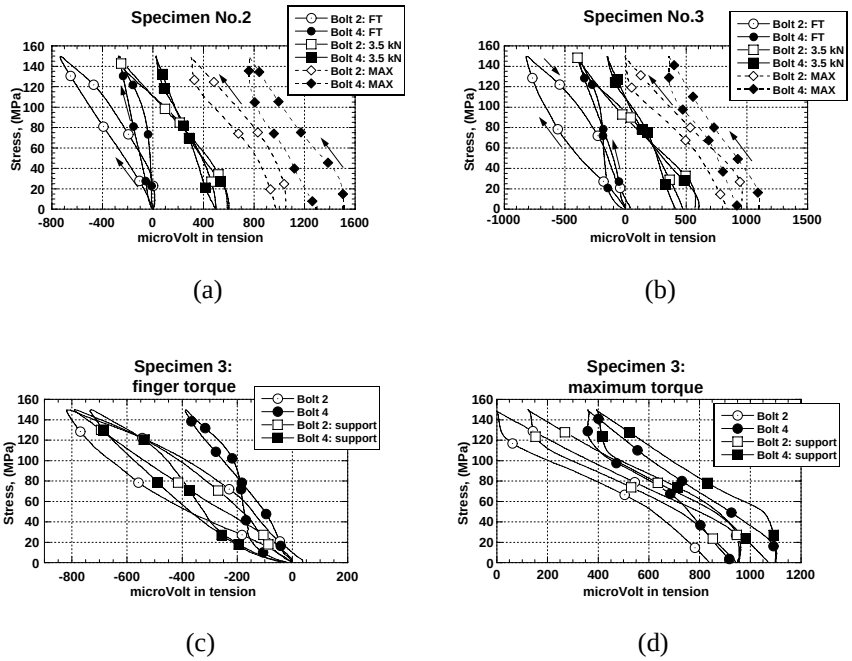

In general, all plots show that the measured axial strain decreased during loading. One of the reasons of this behaviour would be the influence of the Poisson effect in the aluminium plates. The same observation was pointed out in the conclusions of a FEM investigation on composite-to-aluminium single overlap joints [12]. However, this could not have been in the case when the bolts were installed with a finger torque since it did not create any pre-tension in the bolts. This case was not studied in [12]. Therefore, a more realistic reason of the decrease in the axial strain in the bolts is the influence of the contact forces between the joint plates and the bolt shank on the strain gauge measurement in the instrumented bolts (see Fig. 11).

Figure 11. Influence of contact forces on axial measurement in instrumented bolt.

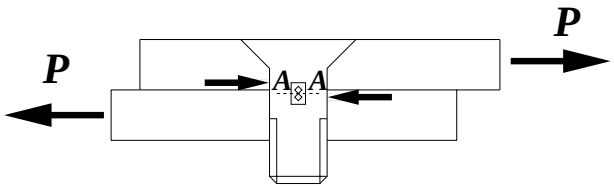

When the load, *P*, is applied to the joint, the shearing contact forces start to act in plane *A–A*, thereby inducing compression there. This affects the axial measurement in the instrumented bolt. The same result was achieved, when the shank of an instrumented bolt was compressed in plane *A–A* using a mechanical wrench. The strain gauges showed negative readings.

As the curves in Fig. 9(c)-(e) show the initial pre-tension in the bolts has dropped during the loading cycle. The initial pre-tension of 3.5 kN in the bolts was achieved each time before to proceed static loading by reassebling the fastener system. In the case of Hi-Lok nuts it was not possible to do it. Therefore, once the Hi-lok nuts had been installed, the specimen

was loaded two times. Figure 9(e) corresponds to the first loading, whereas Fig. 9(f) reflects the second loading. The decrease of the initial pre-tension shown in Fig. 9(c)-(e) could be due to the bolts settling themselves in the bolt holes during the first loading. As Fig. 9(f) shows, there is no decrease in the bolt pre-tension during the second loading.

In addition, as Fig. 9(e) shows, although the same Hi-lok nuts were used on both instrumented bolts, their installation resulted in different initial pre-tensions in the bolts, i.e. pre-loads of 8.1 and 6 kN were achieved in bolts No. 2 and No. 4, respectively. As the plots in Fig. 10(a) and (b) show, the assembly of the instrumented bolts with Hi-lok nuts resulted in bolt No. 4 was more pre-loaded than bolt No. 2. This could be due to the influence of friction between the nuts, the washers, and the plate during the assembly of the fastener system.

Figure 12 shows the shear measurement results obtained on specimen No. 1. The arrows indicate the direction of the curves. Due to a technical problem with the data acquisition system, data were not recorded during the first loading of the specimen with a 3.5 kN pre-tension in the bolts.

Figure 12. Specimen No.1: shear measurement in instrumented bolts.

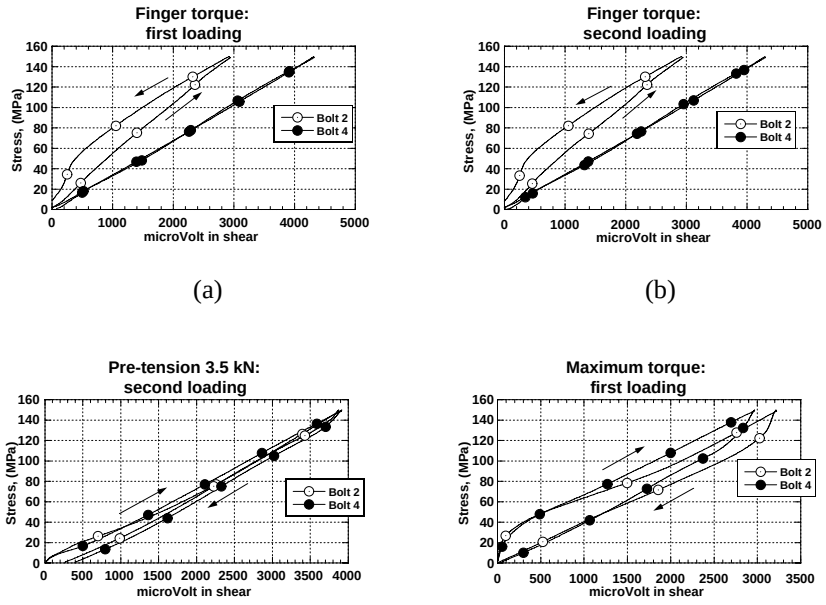

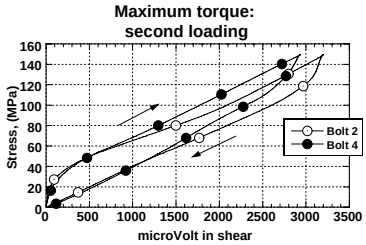

(e)

As the first two plots show, during both static tests, when the bolts were fastened with a finger torque, bolt No. 2 was less loaded than bolt No. 4. When the bolt pre-tension was increased up to 3.5 kN, the bolts transferred almost the same amount of loads. In the case of the Hi-Lok nuts, bolt No. 2 was more loaded than bolt No. 4.

Figures 13 and 14 show the shear measurement results for specimens No. 2 and No. 3, respectively. Specimen No. 3 was tested with and without the anti-buckling support.

Figure 13. Specimen No.2: shear measurement in instrumented bolts.

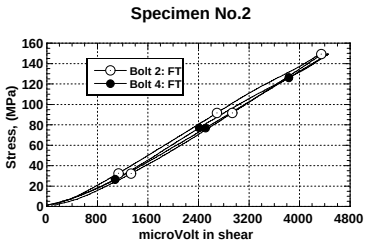

(a)

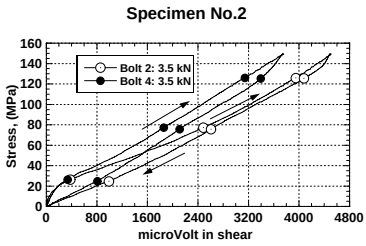

(b)

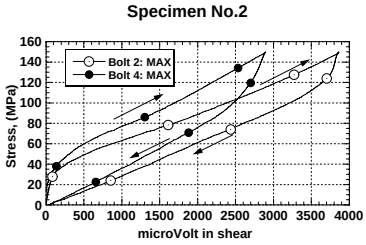

(c)

Figure 14. Specimen No.3: shear measurement in instrumented bolts.

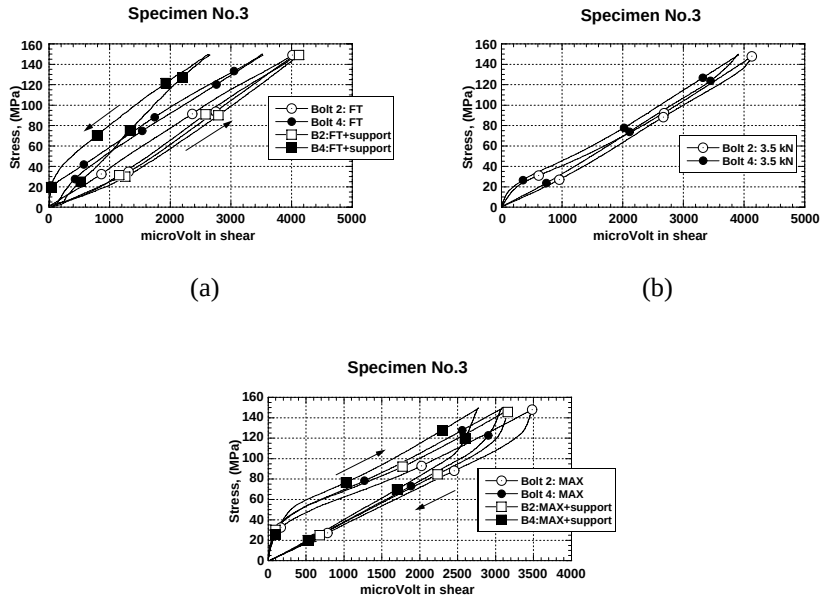

As can be seen, bolt No. 2 was more loaded in shear than bolt No. 4 in most cases. The higher pre-tension was created in the bolts, the more applied load was transferred by the friction forces between the joint parts. As a result, the instrumented bolts with the highest pre-tension measured less shear deformation at the maximum load than in those cases, when the bolts were installed with either a finger torque or pre-tension of 3.5 kN.

As Fig. 14 shows, the use of the anti-buckling support caused a more evident influence of the friction forces on the shear measurement in the bolts with the maximum pre-tension. As a result, the maximum shear deformation measured at the maximum load was less than in the case when the support was not used.

3.2.2 Secondary bending

Secondary bending of the joint plate, SB, was measured using the strain gauges which were located on the same position on both outer and faying surfaces (see Fig. 2). Figure 15 shows the measurement results from two pares of strain gauges, which were located between the two bolt rows and on the plate centre line, SG4/SG17 and SG6/SG18, plotted for specimen No. 1.

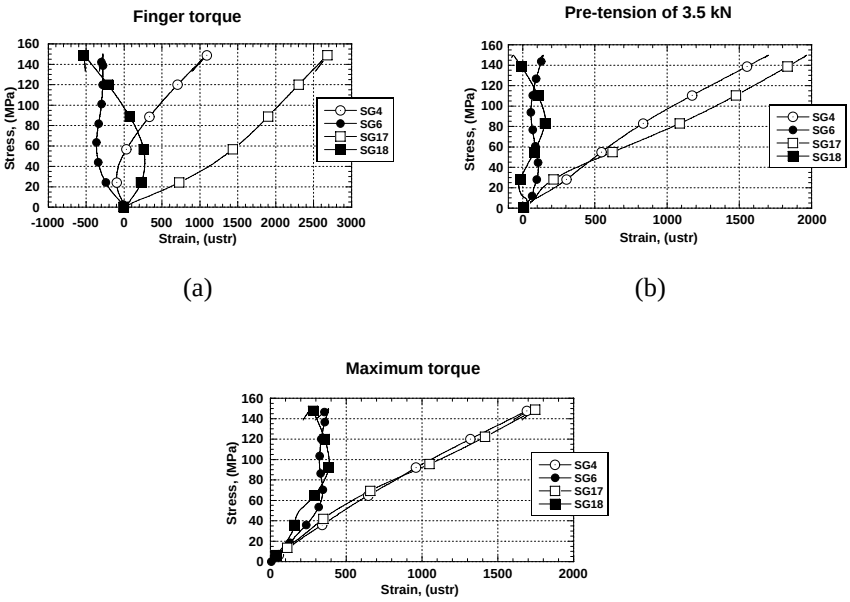

Figure 15. Specimen No.1: strain measured on strain gauges SG4/SG17 and SG6/SG18.

As the SG4 and SG17 curves in the plots show, the initial pre-stress in the bolts affects very much the strain gauge measurements. The higher the initial pre-tension is, the less difference in the measured strain on both strain gauges is observed. Since strain gauges SG6 and SG18 were located between two bolts, their measurement were affected by the bolt behaviour in the bolt holes during loading. Although the specimen was loaded in tension, the strain gauge curves do not show any positive increment in the measured strain. This is due to the contact forces from the bolts compressing the area where the strain gauges were located. It can be seen that, as the initial pre-tension increased, the measured strain shifted slightly towards to the positive values. This is caused by the more influence of the friction force between the plates on the load transfer as the clamping force in the bolts was increased.

Figure 16 shows the measurement results for the same strain gauges obtained on specimen No. 3, where Fig. 16(b) and (d) corresponds to strain gauge measurement when the specimen was tested with the anti-buckling fixture.

Figure 16. Specimen No.3: strain measured on SG4/SG17 and SG6/SG18.

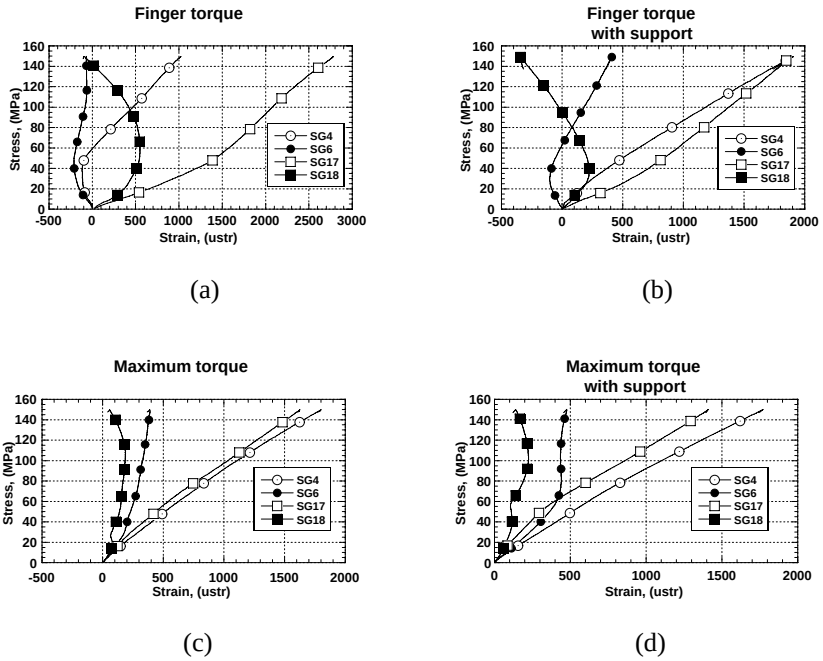

As the strain gauge curves for those tests, when specimen No. 3 was loaded without the support, show their behaviour looks very similar to the corresponding curves for specimen No. 1. In the case when the lateral support was used, as the SG4 and SG17 curves show, there was less difference in the strain gauge measurement than in the case when the specimen was tested without the support. Therefore it seems that the use of the anti-buckling fixture provides more uniform stress distributions through the thickness of the aluminium plate. However, for those tests when the specimen plates were fastened with the highest pre-tension in the bolts, the use of the support did not affect the strain measurement so much (see Fig. 16(c) and (d)).

Figure 17 presents the measured data collected on strain gauges SG10/SG15 and SG11/SG16 on specimen No. 1.

Figure 17. Specimen No.1: strain data collected on strain gauges SG10/SG15 and SG11/SG16.

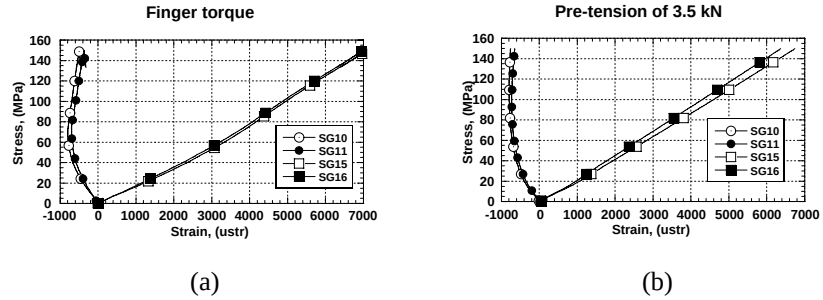

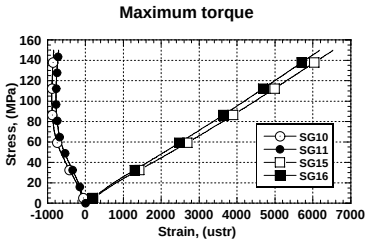

(c)

Those strain gauges, located on the faying surface of the plate, measured almost a linear increase in the strain up to the maximum applied load. As can be noticed, the maximum in the measured strain by these strain gauges decreases as the bolt pre-tension increases, which is due to the influence of the friction forces being more pronounced when the bolts were installed with an initial pre-tension.

However, the strain gauges on the opposite side of the plate showed a different evolution in the measured strain. There is a non-linear decrease in the strain only down to 80 MPa of applied stress. After that the strain gauge curves do not show any change in the strain measured further to the maximum applied load.

The obtained measurement results on strain gauges SG10/SG15 and SG11/SG16 for specimen No. 3, which was tested with and without the anti-buckling support, are shown in Fig. 18.

Figure 18. Specimen No.3: strain measured on strain gauges SG10/SG15 and SG11/SG16.

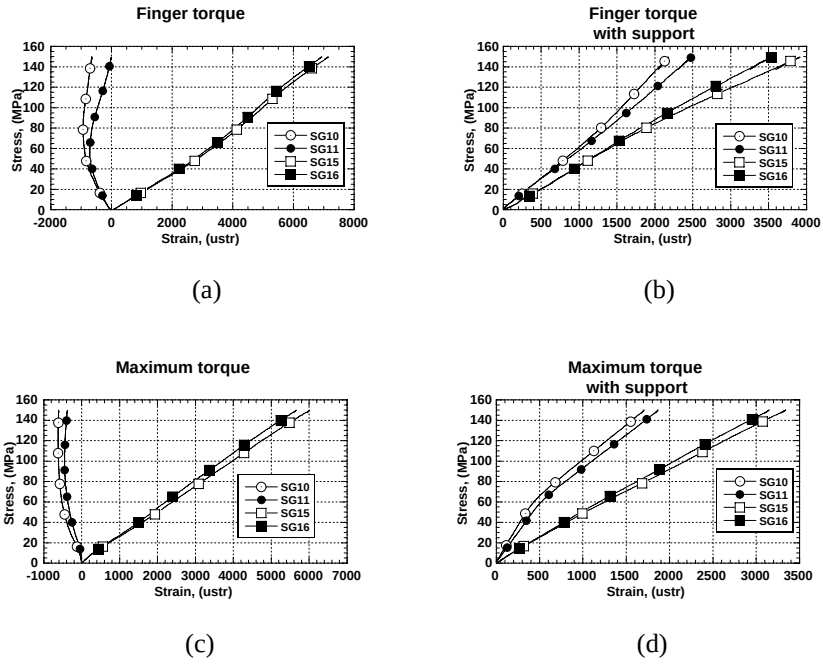

(a) (b)

(c) (d)

As can be seen, the presence of the anti-buckling fixture decreased the absolute difference in the measured strain on the strain gauges located on

both sides of the plate. On the other hand, the maximum strain measured by strain gauges SG15 and SG16 is less when the support is used. This could be due to less influence from secondary bending on the strain gauge measurement and the higher friction forces acting between the joint parts due to the presence of the support. In addition, from an analyse of the strain data in Fig. 18(b) and (d), it can be seen that when the initial pre-tension in the bolts was increased up to the maximum using the Hi-lok nuts, all strain gauges measured less strain deformation than in the case of the bolts being assembled with a finger torque. This is again due to more load is transferred by friction between the plates at high clamping forces in the bolts, which affected the strain gauge measurement.

The obtained results shown in Figs. 15-18 can be represented using the following equation [7]:

$$SB = \frac{\varepsilon_f - \varepsilon_u}{\varepsilon_f + \varepsilon_u}, \tag{1}$$

where ε_f is the strain measured on the faying surface and ε_u is the strain measured on the upper surface of the plate. Figure 19 shows only those values of the calculated secondary bending, *SB*, which correspond to the maximum applied load.

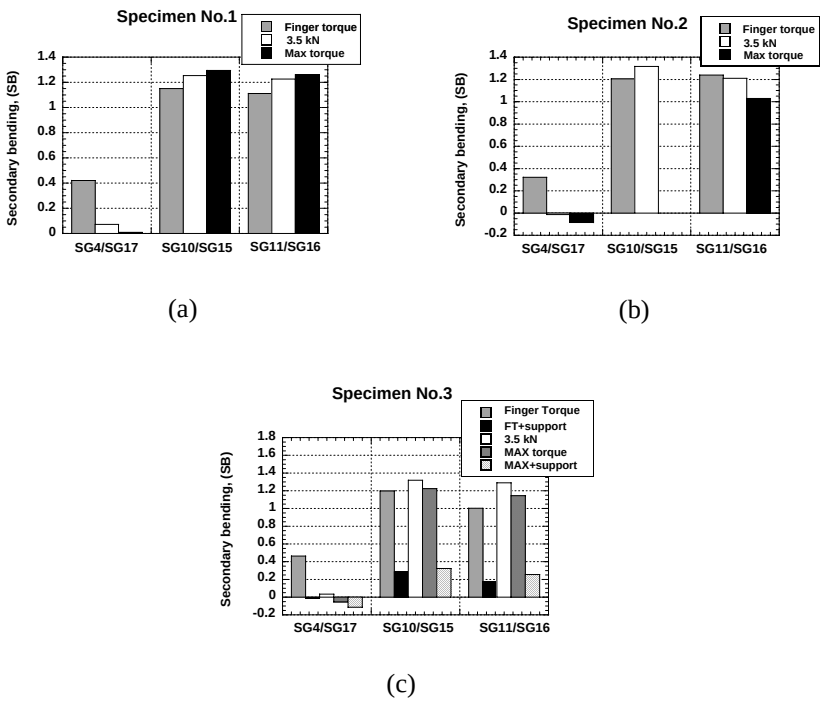

Figure 19. Comparison of measured secondary bending depending on the initial pre-torque in bolts.

As can be seen, secondary bending based on the strain measurement on strain gauges SG4 and SG17 decreased as the initial pre-torque increased, which can be explained clearly by the corresponding strain curves in Figs. 15-16. As the calculated results for SG10/SG15 and SG11/SG16 show, there is no clear relationship between the degree of secondary bending and the

initial pre-tension in the bolts for these strain gauges. Moreover, as the shown results suggest, secondary bending was less in the joint overlap area between the bolt rows, i.e. where strain gauges SG4 and SG17 were located. This could be due to the nature of secondary bending of single overlap joints, when this joint area becomes more consolidated than the area where strain gauges SG10/SG11 and SG15/SG16 are located. This is even more evident when the initial pre-tension in the bolts is increased. Yet, as the calculated results of secondary bending in Fig. 19(c) suggest, secondary bending can be decreased drastically when the anti-buckling support is used.

An alternative illustration of the influence of the lateral fixture and initial pre-torque on the strain measurement is shown in Fig. 20. Here, the two curves show how different pre-tension in the bolts and the presence of the support affected the strain measurement on strain gauges SG4, which was located between the bolt rows, and SG12 placed at the end of the overlap (see Fig. 2).

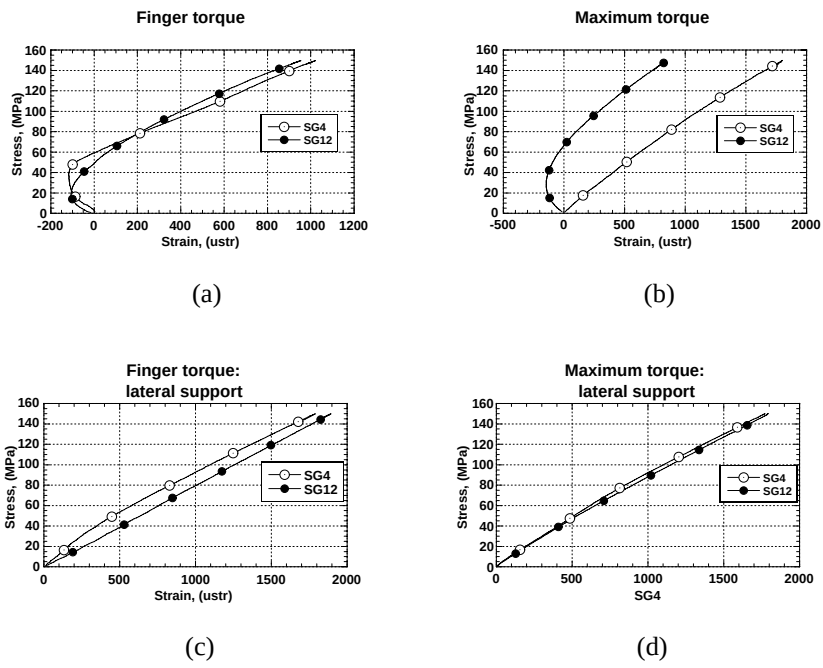

Figure 20. Specimen No.3: comparison of strain measured on strain gauges SG4 and SG12.

As seen, the most non-linear behaviour of the curves corresponds to that test, when the specimen plates were fastened by the bolts with a finger torque; whereas the most linear behaviour, shown by the strain gauge curves in Fig. 20(d), was experienced, when the specimen was loaded with the anti-buckling support being mounted and the joint plates were fastened with the maximum pre-tension in the bolts.

3.2.3 Strain distribution

Figure 21 shows strain distributions on the outer surface across the plate width for specimen No. 1. The obtained measurement results of the strain gauges are plotted as a function of their position and zero position corresponds to the specimens edge, where strain gauge SG13 is located in Fig. 2.

Figure 21. Specimen No.1: strain distribution plots.

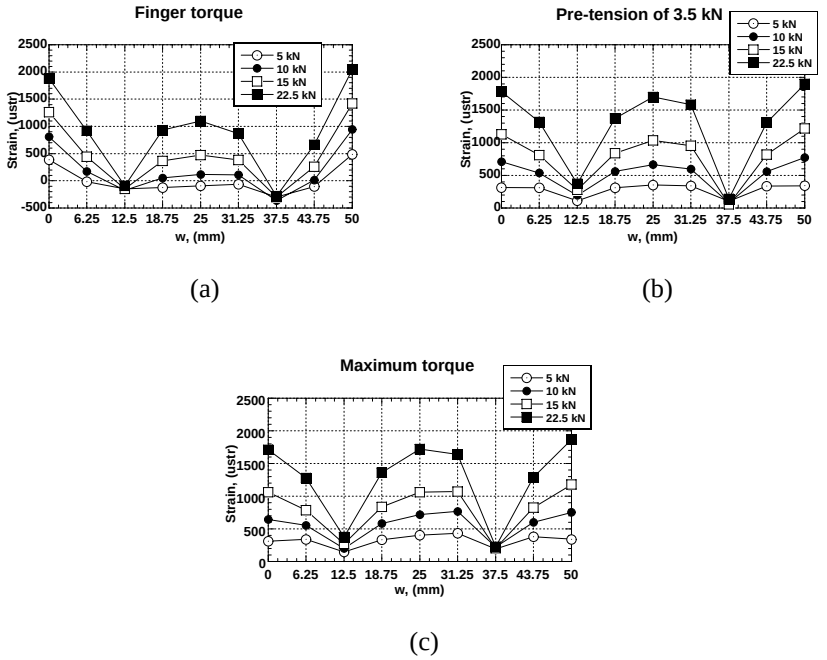

At the beginning of the static test, strain is more evenly distributed than afterwards. This could be explained by the influence of the friction force between the joint plates. Examination of the strain distribution plots in Fig. 21(a) shows the strain maxima at the plate edges, $w = 0$ mm and $w = 50$ mm. It should be taken into account that the corresponding strain gauges are located on the plate edges. Moreover, these strain gauges do not show a similar measurement result in comparison with that strain gauge located in the middle of the plate. This could show how the event of secondary bending affected the strain measurement (see Fig. 22).

Figure 22. Specimen No.3: Measurement on strain gauges SG3, SG17, SG13, and SG14.

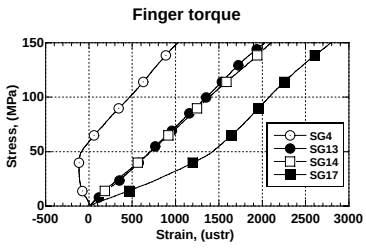

Due to secondary bending, there would be a linear strain distribution through the joint thickness. The strain gauges, glued on the plate edges, measured

strain on a half of the joint thickness, i.e. the measured strain should be an average between those strains measured on the top and faying surfaces. This is illustrated by the corresponding strain gauge curves in Fig. 22.

The minimum in the strain distribution plots corresponds to those strain gauges, which were located between two bolts. The influence of the contact forces from the bolts is the cause of the strain minimum (see the SG6 and SG18 strain gauge curves in Figs. 15-16).

The strain distribution plots for the other two pre-tension levels show a new maximum in the strain distribution, that is at the middle of the joint plate (w = 25 mm), along with those ones on the plate edges. This indicates a more uniform strain distribution through the plate thickness in the overlap area as the bolt pre-tension was increased. As can be noted, there is almost no difference in the stress distribution in the plots for pre-tension of 3.5 kN and those ones for the maximum torque (see Fig. 21(b) and (c)).

The measured strain distributions for specimen No. 3 tested with and without the anti-buckling fixture are shown in Fig. 23.

Figure 23. Specimen No.3: strain distribution plots.

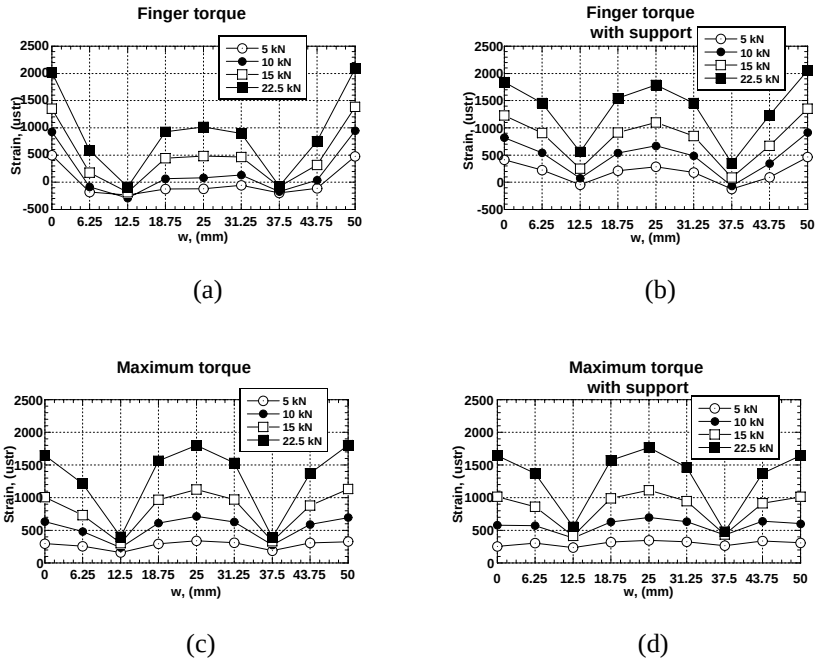

Comparison of the first two plots, see Fig. 23(a) and (b), points out the substantial influence of the lateral support on the strain distributions. In the case when the anti-buckling fixture was used, there is no difference in the strain measured at the hole edges and at the middle of the top plate.

Examination of the next two plots, see Fig. 23(c) and (d), shows that the combination of the maximum pre-tension in the bolts and the use of the fixture did not result in any additional improvement in the strain distribution. As seems, the maximum pre-tension in the bolts, without having the lateral support, significantly reduced secondary bending in the overlap area of the joints.

3.2.4 Load transfer

The ratio of load transfer, LT, was calculated by integrating the strain distribution measured by strain gauges located between the bolt rows using Simpson's formula [17]. It is determined as a ratio of load transferred by each bolt row and the applied load to the inspected plate. The load-transfer calculations were performed only for those joints which were tested with 3.5 kN and full pre-torque since secondary bending of the joint was minimal in these cases (see Fig. 19). The calculation results of the LT-ratio for the bolted joints are presented in Figs. 24-26. In the discussion, the top bolt row with bolts Nos. 1 and 2 in Fig. 4(b) is further referred as "first bolt row"; whereas the bolt row with bolts Nos. 3 and 4 is further named as "second bolt row".

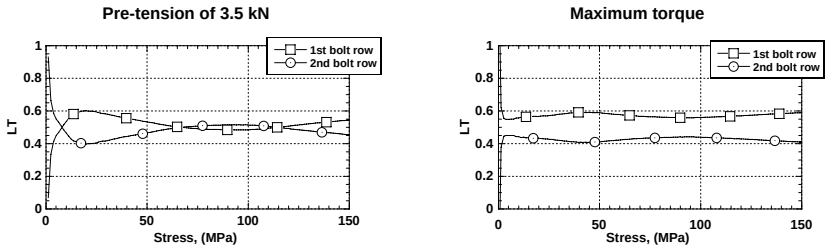

(a) (b)

Figure 24. Specimen No.1: distribution of applied load between bolt rows.

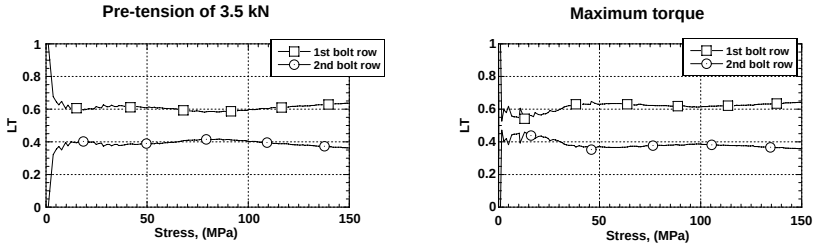

(a) (b)

Figure 25. Specimen No.2: distribution of applied load between bolt rows.

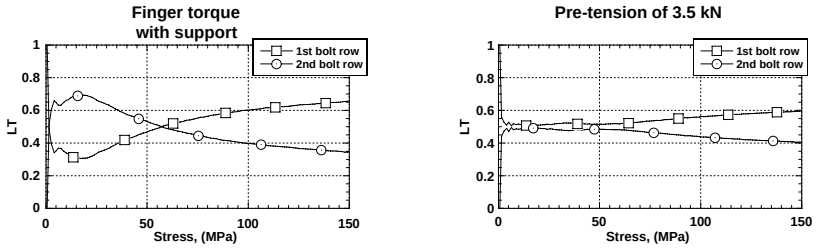

(a) (b)

Figure 26. Specimen No.3: distribution of applied load between bolt rows.

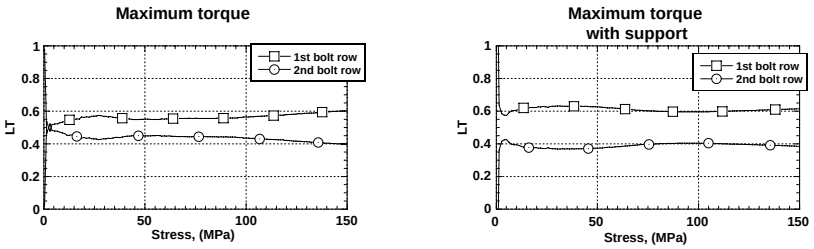

(c) (d)

As the LT-curves show, in most cases the first bolt row transferred up to 60% of the applied load. Moreover, there is no influence of the initial pre-tension on the distribution of applied load between the bolt rows when the bolts were installed with either 3.5 kN or full pre-tension since the LT-curves show the same distribution of the applied load. However, as was already pointed out, high levels of the initial pre-tension decrease drastically secondary bending in the joint overlap, thus providing a more uniform strain distribution through the thickness of the inspected plate.

Examination of the LT-plots in Fig. 26(c) and (d) shows the same distribution of the applied load in the cases when the specimen was tested without and with the anti-buckling support being mounted. It is not clear, therefore, that there is any significant effect of the use of the support on the load transfer. However, as was already noted, high levels of the initial pre-tension in the bolts reduce secondary bending in the overlap region only; whereas the use of the anti-buckling support decreases secondary bending along all length of the specimen (see Figs. 19 and 20).

The shear measurement results obtained on the instrumented bolts can also be used to calculate and analyse the load transfer in the tested joints. Figures 27–29 present the calculated load-transfer distribution between different bolts and friction.

Figure 27. Specimen No.1: load transfer based on shear measurement in instrumented bolts.

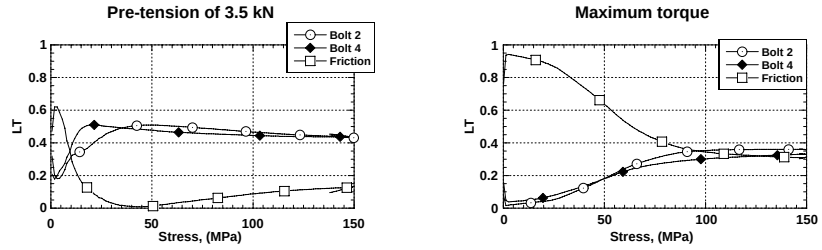

(a) (b)

Figure 28. Specimen No.2: load transfer based on shear measurement in instrumented bolts.

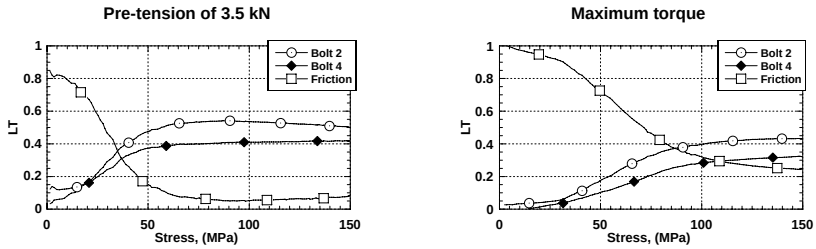

(a) (b)

Figure 29. Specimen No.3: load transfer based on shear measurement in instrumented bolts.

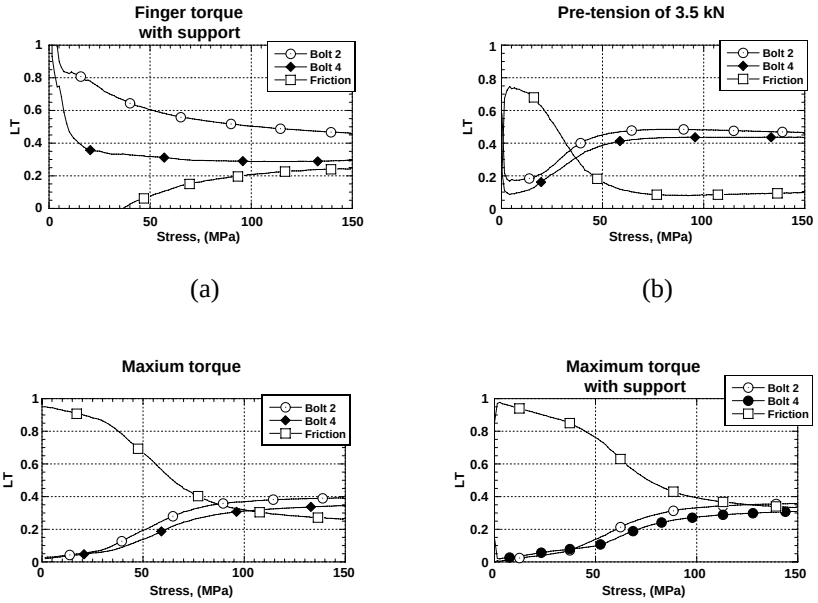

(a) (b)

(c) (d)

As the LT-plots for the case of 3.5 kN pre-tension show, the redistribution of the applied load between the bolts and the friction forces was up to 30-40 MPa of applied stress. After this the bolts carried between 85 and 90% of the applied load and the rest of load was transferred by friction between the joint parts. Moreover, as the bolt LT-ratio plots show, bolt No. 2 from the first bolt row transferred more load than the bolt from the second bolt row. The same distribution of applied load between the bolt rows was shown by the LT-plots based on the strain gauge measurement. When the bolts were assembled with the Hi-Lock nuts, the initial pre-tension in the bolts increased. Since there is a direct relationship between an initial amount of pre-tension in the bolts and the influence of the friction force between the joint plates on the load transfer, the LT-plots in Figs. 27(b), 28(b), and 29(c) show that the load transfer by friction was dominating up to 100 MPa of applied load. As the LT-curves show further, in two cases, see Figs. 27(b) and 29(c), the applied load was equally distributed between the bolts and friction. In the case of specimen No. 2, see Fig. 28(b), approximately

25% of the applied load was transferred by friction when the specimen was subjected to the maximum applied load. Examination of the bolt LT-curves show that bolt No. 2 from the first bolt row was more involved into the load transfer than bolt No. 4 from the second bolt row, which agrees with the LT-results based on the strain gauge measurement.

Examination of the LT-plots for the tests done with and without the anti-buckling fixture, see Fig. 29(c) and (d), shows that the use of the support resulted in more friction was involved into the load transfer. When the specimen was tested without the support, approximately 25% of the applied load was transferred by friction; whereas in the case when the support was used, the friction forces carried approximately 35% of the applied load. However, since these results are based on one test, an additional experimental work might be needed in order to approve them.

Looking at both methods of the load-transfer analysis, one based on the strain gauge measurement and that involving the application of instrumented bolts, the first one seems to be less informative since it presents a general picture of how the applied load is distributed between the joint bolt rows, meaning that the influence of friction is already taken into account. The use of instrumented bolts lets perform a more accurate analyse of the load transfer since it allows to measure the distribution of applied load between each joint member and friction in particular.

3.2.5 Optical measurement

Bolt bending and bolt rotation were measured using Digital Speckle Photography (DSP) method. Figure 30 shows an example of bolt-movement measurement done on bolt No. 1 from specimen No. 1 joined with a finger torque in the bolts.

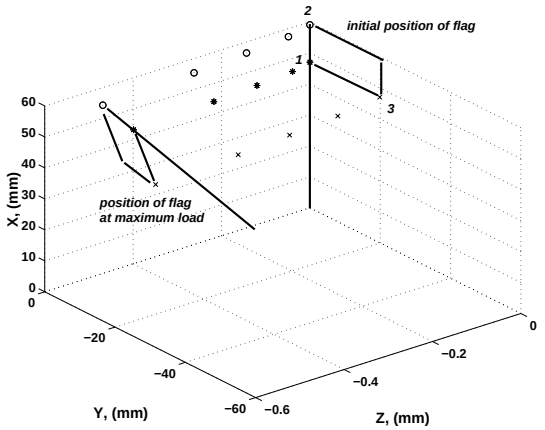

Figure 30. Illustration of bolt movement.

The bolt displacement is based on the dislocation of points *1*, *2*, and *3* located on the flag (see Fig. 4(b)). The positions of the points were taken at different load levels during loading and unloading. In Fig. 30 the loading stage up to the maximum applied load level is presented. As can be seen,

the end of the flag, which was glued to the bolt head, changed the initial position during loading (see Fig. 31(a)).

Figure 31. Illustration of bolt movement: (a) bolt bending; (b) bolt rotation.

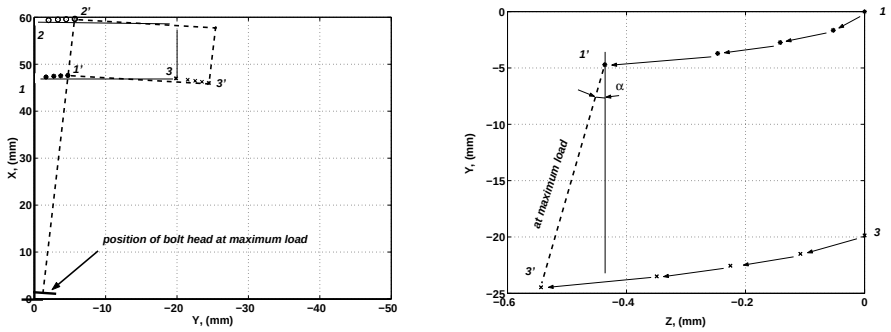

(a) (b)

This was due to the out-of-plane deflection of the specimen that occurred during loading. During bolt-movement measurements the relative displacement between the aluminium plate and the flags was not taken into account. Since secondary bending is found to have been influencing the measurement of bolt movement in the plane *XY*, the obtained results may represent only a relative picture of bolt movement in this plane. In order to calculate bolt movement in the plane *XY*, the measured displacements of point *(1)* were used (see Figs. 4(b) and 31(a)). Figure 32 presents the calculated bolt movement for the tested joints.

Figure 32. Measured bolt movement in *XY* plane.

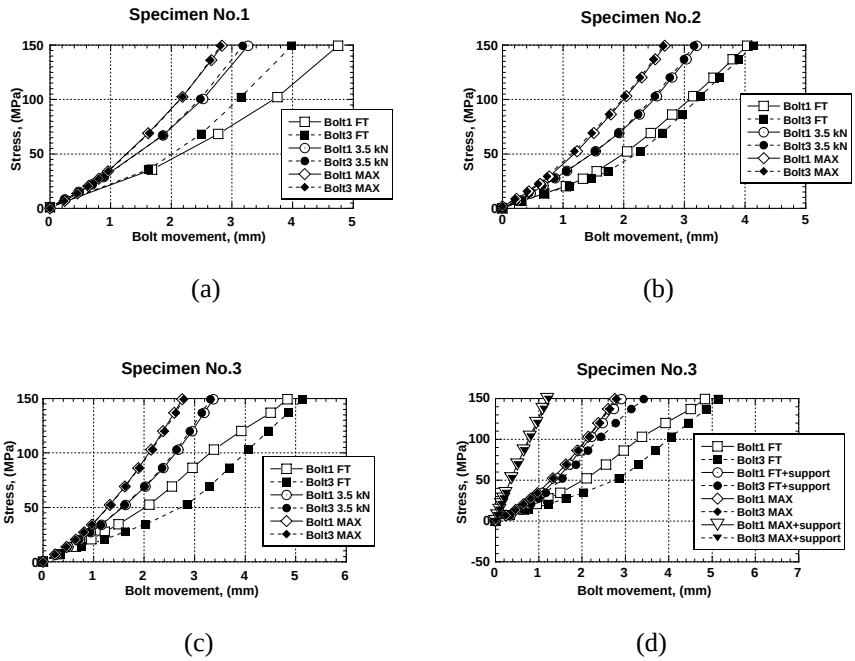

(a) (b)

(c) (d)

As the bolt-movement curves show, there is a relationship between the measured bolt displacement and the initial pre-tension in the bolts for all

specimens. The higher pre-tension in the fasteners was, the less bolt movement was measured. This was due to the higher influence of friction on the load distribution between the joint parts at high levels of pre-tension in the bolts. The higher initial pre-torque was, the more load was transferred by the friction forces, and as a result the bolts were less loaded, which affected directly their movement during loading.

Further examination of the curves shows that bolt movement measured for the same pre-tension level on the different joints was more or less the same. In the case of a finger torque, as shown in Fig. 32(a) and (c), different displacement of bolts No. 1 and No. 3 was measured. However, the same bolts performed almost the same amount of displacement while specimen No. 2 was tested (see Fig. 32(b)). For other pre-tension levels, the measured bolt movement on both bolts was more or less the same. As the plot in Fig. 32(d) shows, the use of the anti-buckling support resulted in less bolt movement than was measured on the bolts when the specimen was tested without the support. On one hand, the anti-buckling fixture induced more load transfer by the friction forces, thus the bolts were less loaded, and as a result they performed less movement. On the other hand, the use of the lateral support resulted in lower secondary bending than in the tests done without the support. As was pointed out above, secondary bending, inducing the out-of-plane deformation of the specimen, could affect the bolt-movement measurement in the *XY*-plane.

Bolt rotation is another event in bolt displacement, which may take place during loading of the bolt (see Figs. 4(b) and 31(b)). It can be calculated using the measured displacements of points *1* and *3* and the following equation:

$$\alpha = \arctan \frac{z'_3 - z'_1}{y'_3 - y'_1}, \tag{2}$$

where α is the angle of bolt rotation in Fig. 31(b); y'_1, y'_3, z'_1, and z'_3 are the *Y* and *Z* coordinates of points *1* and *3* measured at the maximum applied load (see Fig. 31(b)). The calculated results of bolt rotation are presented in Fig. 33.

Figure 33. Measured bolt rotation in *YZ* plane.

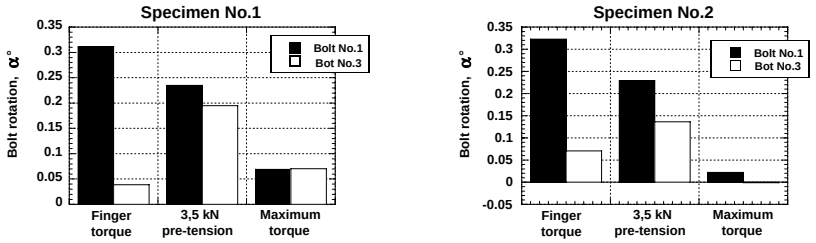

(a) (b)

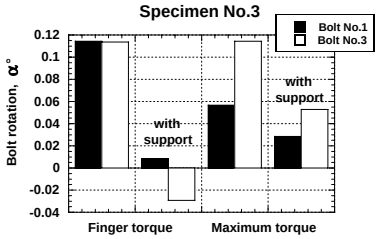

(c)

In Fig. 33 the first two plots show that an increase in the bolt pre-tension lowered rotation of the bolts. As has already been mentioned, an increase in the bolt pre-tension resulted in the bolts were less loaded since a larger part of the applied load to the specimen was transferred by the friction forces. On the other hand, the bolts mounted with an initial pre-tension are less prone to rotation than the bolts assembled with a finger torque since the friction forces between the fastener system and the plates are higher when a certain pre-tension in the bolts exists. As both plots show, in most cases bolt No. 1 performed more rotation than bolt No. 3.

Figure 33(c) shows the obtained results on bolt rotation for specimen No. 3 tested with and without the lateral support. As seen, the use of the support decreased bolt rotation as well as an increase in the bolt pre-tension. However, in comparison with the first two joints, in specimen No. 3 rotation measured on bolt No. 3 was larger than for bolt No. 1. This could be due to the bolts installed with a different pre-tension although the same type of Hi-Lok nuts being used. As the axial measurement results from the instrumented bolts have shown, after the bolt assembly a different axial pre-tension was measured in both bolts (see Figs. 9(c) and 10(a) and (b)). This should result in different friction between the fastener system and the plates, which would affect bolt rotation of different bolts.

3.3 Spectrum tests

3.3.1 Tested joints

The specimens were tested in spectrum according to the experimental programme specified in Table 3. After the spectrum tests, the joints, which were subjected to 20 and 60 FALSTAFF blocks, were visually inspected for the presence of any visible damage. The faying surfaces of the joint plates were subjected to wear and fretting during testing. Figure 34(a)-(d) shows the faying surfaces of the plates for both joints.

(a) plate with countersunk holes

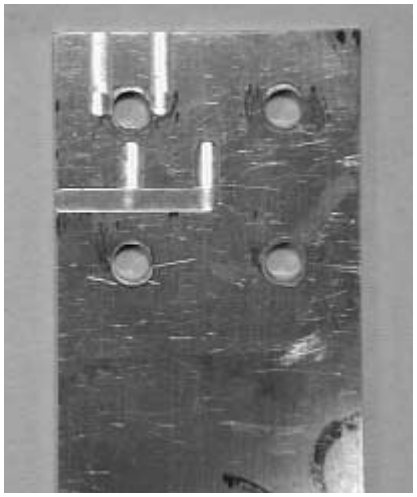

(b) plate with ordinary holes

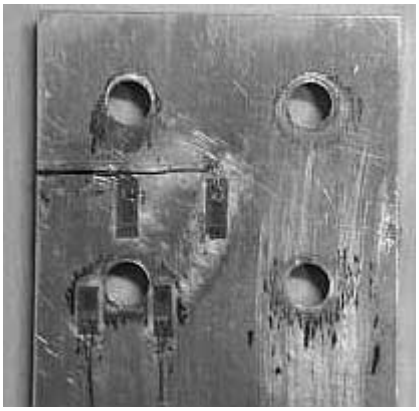

(c) plate with countersunk holes

(d) plate with ordinary holes

Figure 34. Plates of tested joints: (a) and (b) 20 FALSTAFF blocks; (c) and (d) 60 FALSTAFF blocks.

As examination of the faying surfaces shows, there are areas of wear around the bolt holes, which indicate fretting wear between the contact surfaces of the aluminium plates. Moreover, the size of the worn areas is larger for that joint, which was subjected to 60 spectrum blocks.

The third joint was supposed to be subjected to spectrum loading until any visible crack would be observed on the plate surface, that was estimated to take place after 120 FALSTAFF blocks in the course of previous spectrum testing of aluminium joints with the same geometry and configuration [10]. However, the joint broke after 105.13 FALSTAFF blocks as shown in Fig. 35(a), i.e. net-section failure had occurred in the plate with ordinary holes.

Figure 35. Joint broken after 105.13 FALSTAFF blocks (a). Faying surfaces of the joint plates (b) and (c).

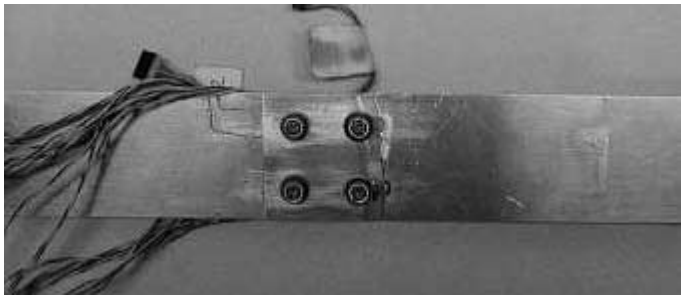

(a)

(b) plate with countersunk holes

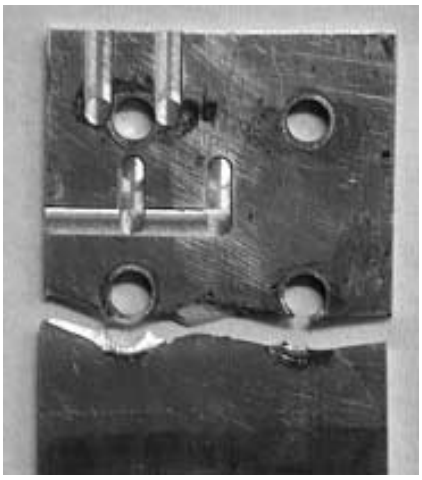

(c) fractured plate with ordinary holes

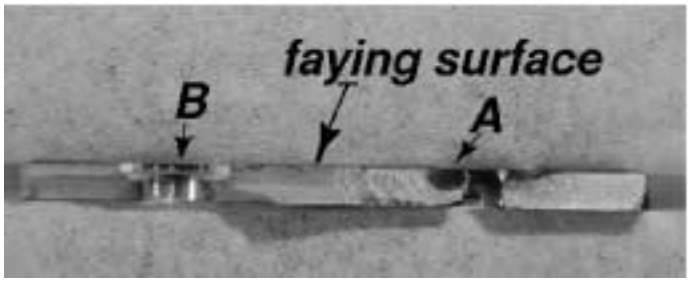

(d)

During the last visual inspection after 95 blocks no damage formation was observed in the specimen from outside. The faying surfaces of both plates are presented in Fig. 35(b) and (c). As visual observation of the fracture surface showed, the cause of the fracture was a fatigue crack nucleated from the faying surface of the plate with ordinary holes. Moreover, a more detail examination shows that the crack initiated at a certain distance away from the edge of bolt hole No. 1. This location is typical for aluminium joints bolted by fastener systems with high clamping forces since the fretting mechanism is recognized as dominant in the nucleation of fatigue cracks [1, 3].

The site of the crack propagation is shown by a visible black area (see mark *A* in Fig. 35(d)), which reflects the fact that the crack was filled in by oxide debris. A similar nucleation site of another crack is observed near bolt hole No. 2 (see mark *B* in Fig. 35(d)). This evidences the transition from fretting wear to fretting fatigue, when one or more surface microcracks initiated due to the near-surface plastic deformation in the contact surfaces transform into a fatigue crack, which propagats into the bulk material [1].

3.3.2 Grip displacement

The grip displacement, corresponding to the peak to peak elongation of the specimen during one acquisition cycle recorded after a different number of spectrum blocks, is presented in Fig. 36.

Figure 36. Specimen elongation plots.

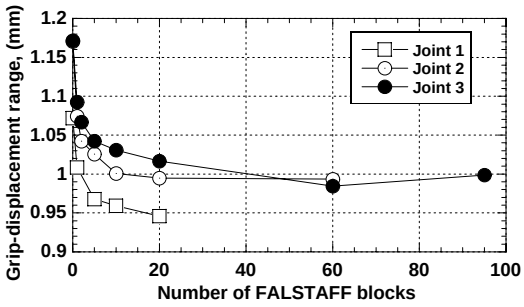

As the plot shows, during the first stage of spectrum loading there is a drastical decrease in the relative displacement between the aluminium plates. According to Ref. [1], at the beginning of spectrum loading the thin oxide layer covering the surface of the joint plates suffer from degradation due to mechanical wear processes. This leads to the removal of the protecting oxide layer and the origin metal of the contact surface starts to adhere. This results in the initial accumulation of wear debris between the aluminium plates, thus increasing the coefficient of friction of the aluminium material during the first spectrum blocks. As a result, this decreases the relative displacement between the aluminium plates. As the grip-displacement curve for the first joint shows, the spectrum loading of the specimen was com-

pleted (i.e. after 20 FALSTAFF blocks) precisely after this loading stage characterized by the high influence of the wear and fretting processes on the relative displacement of the plates.

The next stage in the degradation of the contact surfaces is associated with additional wear and the potential formation of new oxide, through the oxidation of either wear particles or the origin metal, and near-surface plastic deformation [1]. The latter event can lead to the nucleation of grain-sized surface microcracks. In the specimen elongation plots, their horizontal part corresponds to this stage in the loading history of joints Nos. 2 and 3.

Additional spectrum loading leads to the surface microcracks grow into the bulk material. As they propagate, they could link between each other, forming one or several large cracks. At this stage the further propagation of such cracks is more dominated by global stresses, whereas the influence of the contact stresses is less important [1]. It could be that an increase in the grip-displacement curve for joint No. 3, measured after 95 FALSTAFF spectrum blocks, reflect this damage development in the specimen. This joint broke after 105.13 spectrum blocks.

3.3.3 Measurement in instrumented bolts

The axial and shear deformations of two instrumented bolts were measured after a different number of spectrum blocks as specified in Table 3. Figure 37 shows the axial measurements in the instrumented bolts for the tested joints.

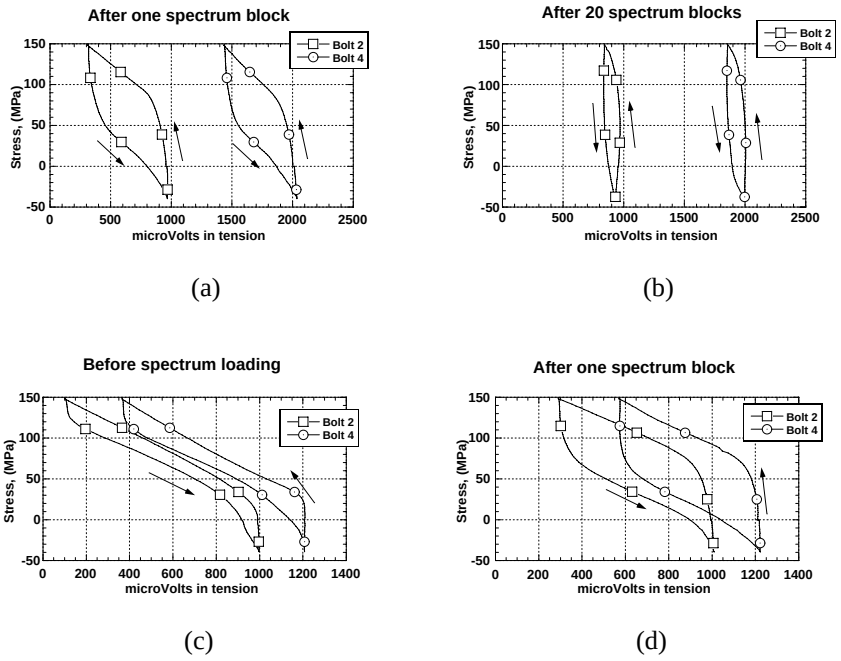

Figure 37. Axial measurements in instrumented bolts: (a)-(b) specimen No.1; (c)-(e) specimen No.2; (f) specimen No.3.

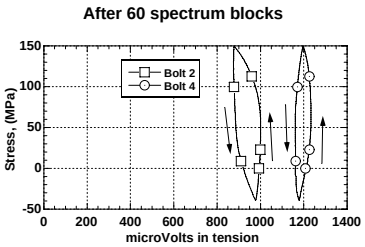

(e)

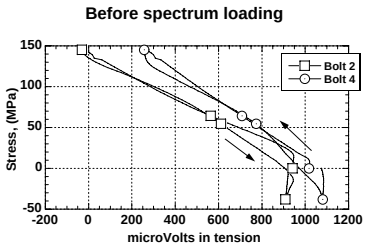

(f)

It has already been pointed out that the contact forces between the bolt shank and the plates affected the axial measurement in the instrumented bolts (see Fig. 11). The obtained results shown in Fig. 37(a), (b), (d), and (e) are a combination of measurement taken during one acquisition cycle and the initial pre-tension measured during the bolt assembly. During spectrum testing before each data acquisition the strain gauges on the instrumented bolts were calibrated. Therefore, it was not possible to see the actual change of the initial pre-tension during spectrum loading. However, it would be possible to do this if the axial deformation of the bolts would have been tracked constantly during the test. In this case, the bolt pre-tension should be taken at zero load after a specified number of spectrum blocks.

Figures 38-40 present the obtained shear measurement results for the instrumented bolts in the joints.

Figure 38. Shear measurements in instrumented bolts for joint No.1.

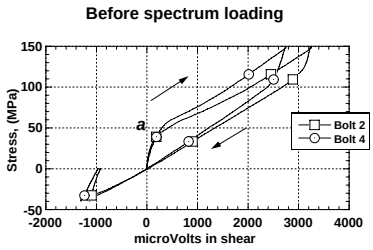

(a)

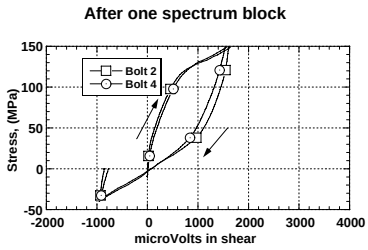

(b)

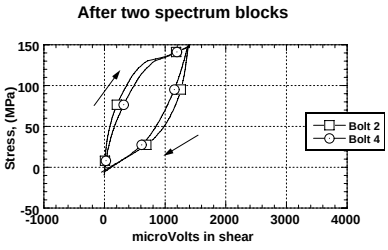

(c)

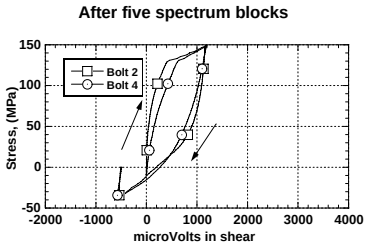

(d)

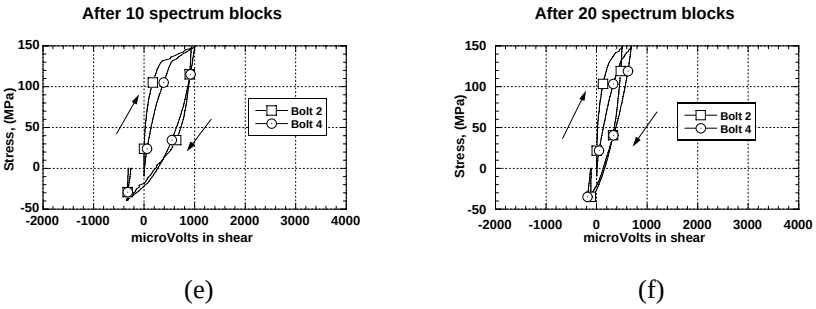

(e) (f)

Figure 39. Shear measurements in instrumented bolts for joint No.2.

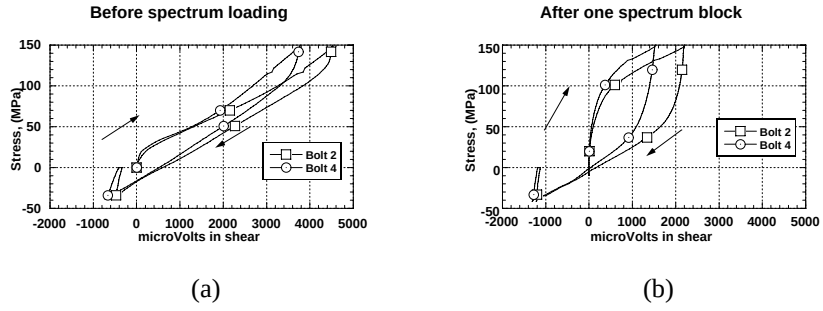

(a) (b)

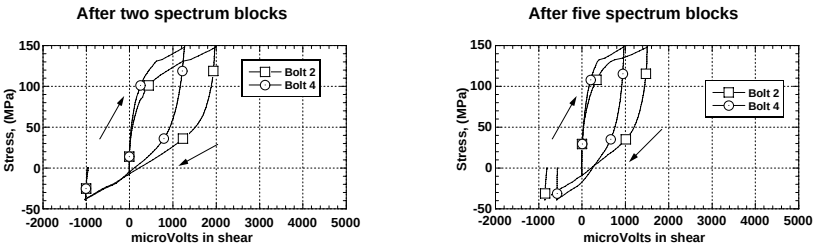

(c) (d)

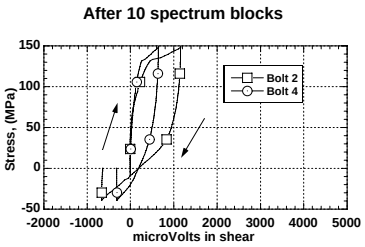

(e)

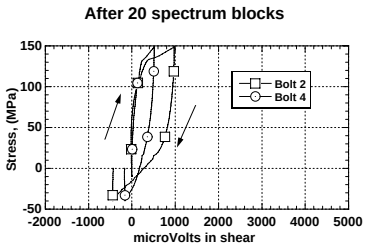

(f)

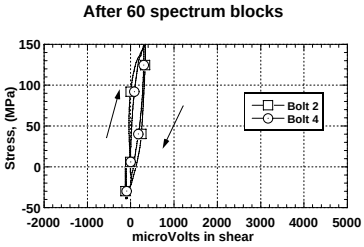

(g)

Figure 40. Shear measurements in instrumented bolts for joint No.3.

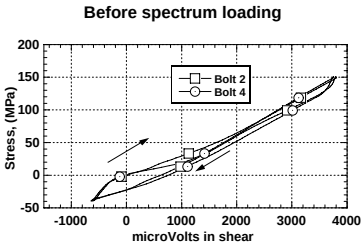

(a)

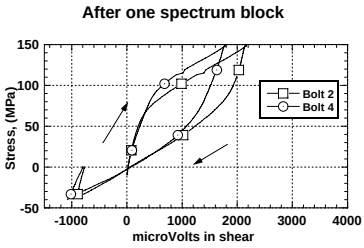

(b)

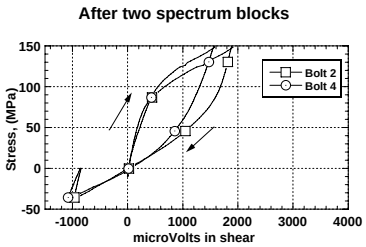

(c)

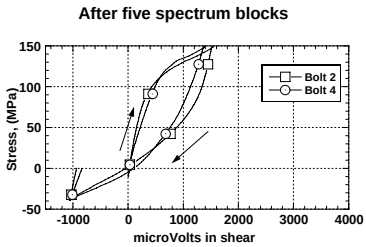

(d)

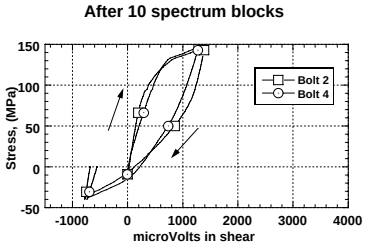

(e)

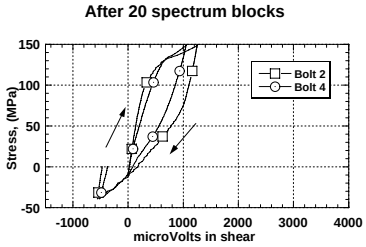

(f)

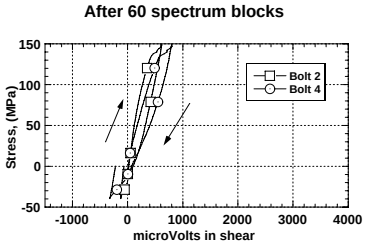

(g)

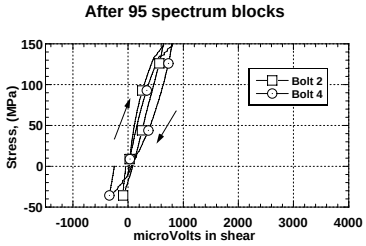

(h)

In general, the plots show the same evolution in the shear response measured after a different number of cycles for all tested joints. As Fig. 38(a) shows, until point *a* the load was mostly transferred by the friction forces between the joint parts. When the friction stage was overcome, the load was carried by the bolts. Moreover, bolt No. 2 was more loaded at the maximum load than bolt No. 4. The unloading part looks almost the same except that at the minimum load both bolts carried the same loads. The next plots in Fig. 38 show a more pronounce influence of the friction forces on the shear measurement in the instrumented bolts after the spectrum loading was started and continued. The increased load transfer by friction resulted in the bolts were less loaded than during the first data acquisition cycle. As the number of spectrum blocks increased, the coefficient of friction between the joint plates became higher, which would increase the friction forces and their influence on the load transfer between the joint parts. The load transfer in the joints is further discussed in details.

3.3.4 Secondary bending

Secondary bending, SB, was calculated after a different number of FALSTAFF blocks for each specimen using Eq. 1. As for the static tests, secondary bending was calculated only for the peak loads. Figure 41 shows the obtained results of SB for the specimens. It should be noted that despite the logarithmic scale used in the plots, the horizontal axis starts from zero, which corresponds to the first measurement before the spectrum loading was started (see Fig. 6).

Figure 41. Secondary bendir after a different number of spe trum blocks.

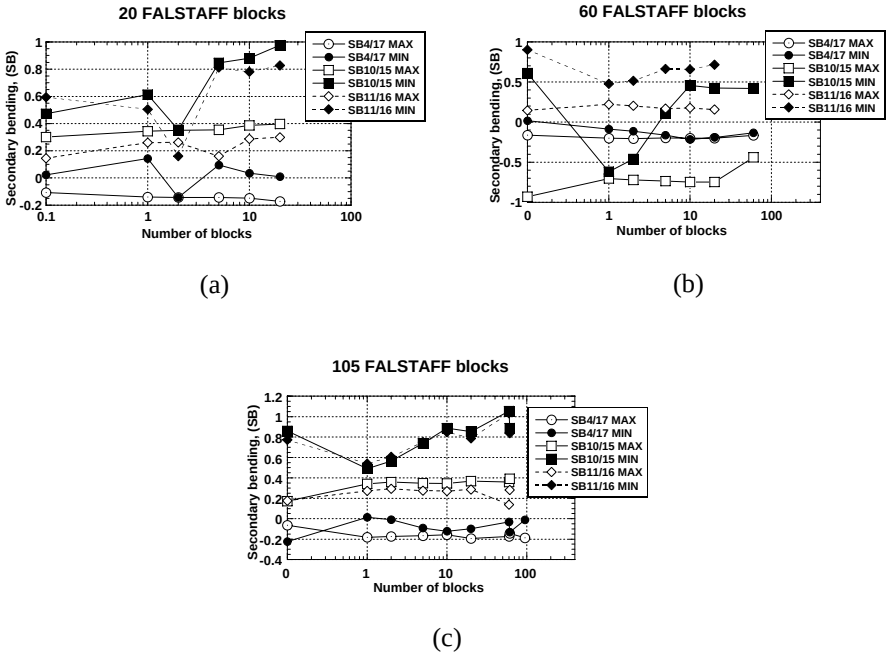

The SB4/17 curves show that secondary bending was similar at the maximum and minimum load peaks. These curves show also that secondary bending measured after a different number of spectrum blocks did not change so much from those values measured before the spectrum loading was applied. This indicates that secondary bending in the joint overlap area was more or less the same during the spectrum tests. When secondary bending corresponding to the measured data on strain gauges SG10/SG15 and SG11/SG16 is considered, it is seen that at the minimum load peaks secondary bending was larger than at the maximum load peaks. Moreover, the curves show that secondary bending at the minimum load peaks increased with the number of spectrum blocks; whereas at the maximum load peaks it rather seems to have been more or less constant. Out-of-plane deformation of the specimens was larger at the negative load since such a loaded joint is more prone to buckling. In addition, a possible decrease in the initial finger torque in the bolts, fastening the support plates, could be the reason of the increased secondary bending at the negative load peaks during the spectrum tests.

3.3.5 Load transfer

The ratio of load transfer, LT, for the bolt rows calculated at the maximum and minimum load peaks after a different number of spectrum blocks is shown in Fig. 42 for the tested joints. It should be noted that despite the logarithmic scale is used in the plots, the horizontal axis starts from zero, which corresponds to the first measurement before the spectrum loading was initiated (see Fig. 6).

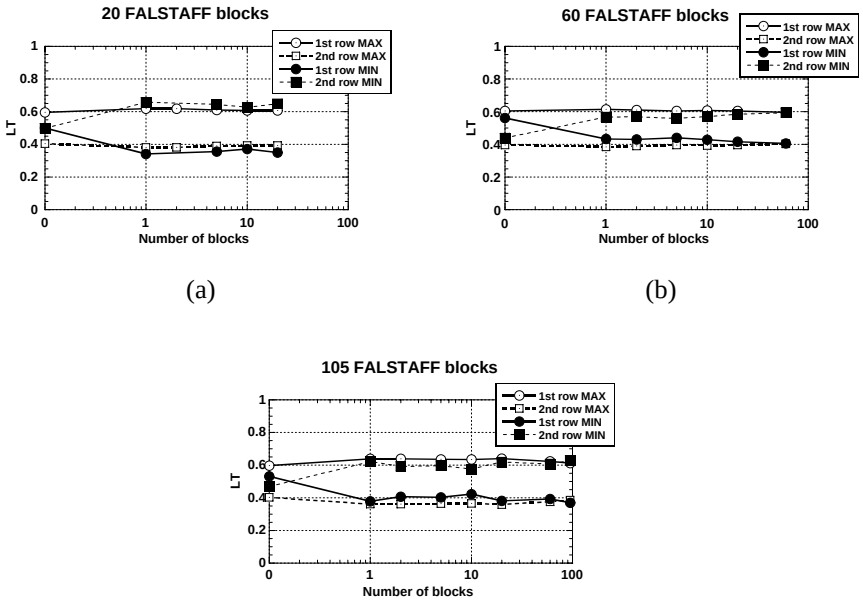

Figure 42. Distribution of applied load between bolt rows after different number of spectrum blocks.

As the LT-ratio plots show, the distribution of the applied load was the same in all three joints. At the maximum load peaks the first bolt row transferred more load than the second bolt row. However, at the minimum load peaks the distribution of the load between the bolt rows was opposite, i.e. the second bolt row was more loaded than the first one. However, during the first measurement done before the first spectrum block was performed, the first bolt row carried more load during both maximum and minimum load peaks. These results agree with those obtained during the static tests and presented in Fig. 24-26 for the cases when the joints were tested with the maximum pre-tension and the lateral support used.

From the grip-displacement plots in Fig. 36, the significant influence of the friction forces on the relative displacement of the joint plates was pointed out. The friction forces, which were increasing during the first twenty spectrum blocks, should affect the load transfer between the bolt rows in the specimen. Since the aforementioned LT-ratio results already include the load transfer by friction, it would be of interest to analyse the influence of the friction forces on the load transfer with help of the shear measurement in the instrumented bolts (see Fig. 43).

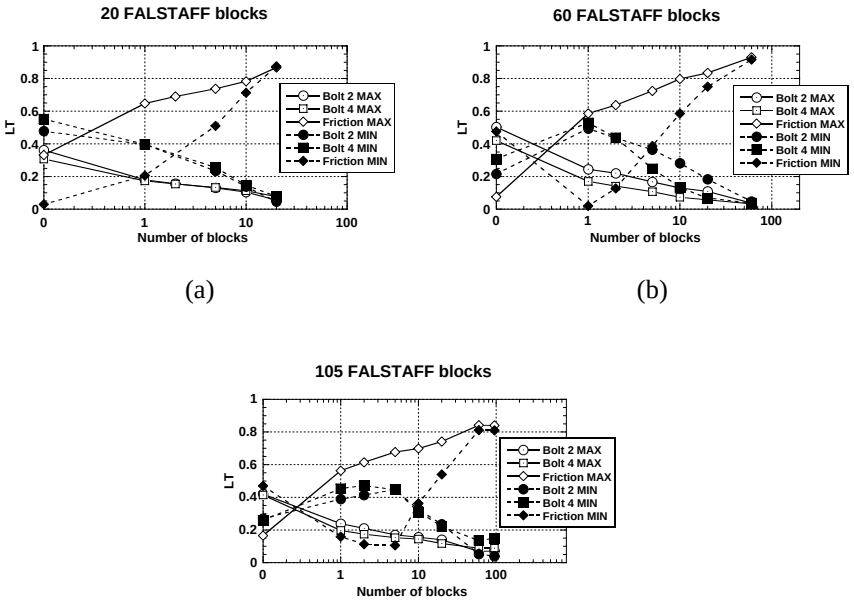

Figure 43. Distribution of applied load between bolts and friction based on shear measurement in instrumented bolts.

As seen, during the first measurement the load was mostly transferred by the bolts. However, this load distribution changed already after the first applied spectrum block. As the number of spectrum blocks increased, the load transfer by the bolts decreased. It can be noted that at the maximum load peaks the load transfer by friction is more dominant than at the minimum load peaks. After 20-60 spectrum blocks, depending on which specimen is considered, the same portion of the applied load was transferred by the friction forces at both maximum and minimum load peaks. At this stage up to 80-90% of the applied load was carried by friction and the rest of it was transferred by the bolts. These results point out the significance of friction in the load transfer during spectrum loading.

3.3.6 Optical measurement

Bolt movement after a different number of spectrum blocks was measured using the optical system. Figure 44 shows the obtained measurement results for the tested joints. They are based on the measured displacements of point *1* in the *XY* plane (see Figs. 4(b) and 31(a)). In the plots the displacement of this point at the maximum and minimum load peaks is presented after a different number of spectrum blocks.

Figure 44. Bolt movement during spectrum loading.

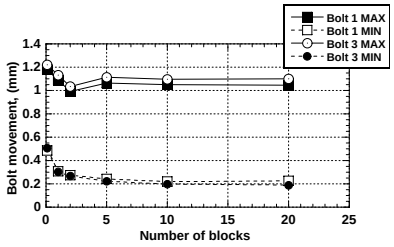

(a) 20 FALSTAFF blocks

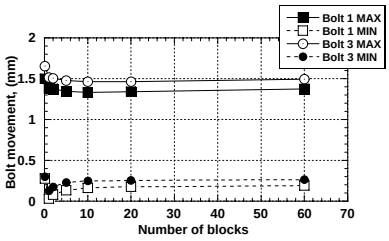

(b) 60 FALSTAFF blocks

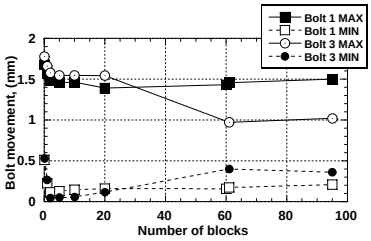

(c) 95 FALSTAFF blocks

The bolt-movement curves can be characterized by three different stages of evolution as well as the aforementioned grip-displacement curves. At the beginning of the spectrum tests, the curves show a decrease in bolt movement. This is due to an increased friction coefficient of the aluminium plates. This was due to fretting wear between the plates. As a result, the friction forces increased resulting in a larger part of the applied load transferred by them. This led to the bolts were less loaded, and thereby their movement decreased.

The next stage of the shown curves is presented by a more or less constant bolt movement measured between 10 and 20 FALSTAFF blocks. This stage may be characterized by the transition from fretting wear to fretting fatigue, when fatigue damage start to nucleate. The last stage in the evolution of the curves is associated with a slow and steady increase in bolt movement measured after 20 FALSTAFF spectrum blocks. This loading stage is believed to be dominated by fatigue damage development in the specimens. A decrease in the bolt-movement curve shown for bolt No. 3, see Fig. 44(c), was caused by the flag on this bolt had been attached to the bolt head since it became unglued after 50 spectrum blocks.

Additional examination of the presented curves shows that the bolt movement measured on bolt No. 3 at the maximum load peaks was slightly larger than that measured on bolt No. 1. However, this is not the case for the minimum load peaks.

4 Conclusions

This report has presented an experimental investigation on the behaviour of single overlap bolted joints tested in static and spectrum loading. Several conclusions gained from the obtained results are summarized below regarding to different subjects of the present study:

Instrumented bolts: The axial measurements in the instrumented bolts were affected by the contact forces between the bolt shank and the plates during loading. Therefore, it would be of interest to study this event in future experimental work. The shear measurements in the instrumented bolts allowed to perform an accurate analysis of the load transfer between different bolt rows and friction forces.

Bolt pre-tension: An initial amount in the bolt pre-tension has a significant influence on the joint performance during loading. The higher pre-tension was in the bolts, the more load was transferred by friction as well as the less secondary bending was observed in the joint, which resulted in more uniform strain distribution through the plate thickness.

Load transfer: The calculation results of the load transfer, based on strain gauge measurements, show that bolt rows transfer a different amount of the applied load. However, this method to analyse the load-transfer distribution does not represent the influence of the friction forces. Those calculation results, which were based on the shear measurement in the instrumented bolts, show that up to 30% of the applied load was transferred by friction during static loading. During spectrum testing, the influence of the friction forces on the load transfer was rather dominating. Due to fretting wear the coefficient of friction increased during spectrum loading, and as a result, a larger part of the applied load was carried by friction.

Secondary bending: Secondary bending depended on the initial amount of pre-tension in the bolt. Joints fastened with a finger torque in the bolts performed the highest out-of-plane deflection, which resulted in a non-uniform strain distribution through the plate thickness. The use of anti-buckling support decreased drastically secondary bending of the joints. The highest torque in the bolts provided less secondary bending in the overlap area only, whereas the lateral support lowered secondary bending along all joint length. Secondary bending in the overlap area was almost the same during spectrum loading, whereas secondary bending, based on strain gauge measurements located at the end of the joint overlap, was larger at the minimum load peaks than that measured at the maximum load peaks.

Bolt movement: The use of Digital Speckle Photography (DSP) method to measure bolt movement allowed to obtained accurate measurement results on both bolt bending and rotation. However, a relative displacement of

the bolt and the plate surface should be taken into account since the out-of-plane deflection of the joint affected the optical measurement. The obtained results on bolt movement show that bolt bending and bolt rotation depend on an initial amount of pre-tension in the bolt. The higher pre-tension was introduced, the less bolt movement was measured. Bolt movement measured during spectrum testing was influenced by friction between the plates and fatigue damage in the joint.

5 Acknowledgements

Mr. Bengt Nyberg is acknowledged for assistance with the laboratory equipment. Help by Dr. Gunnar Melin with the optical measurements is gratefully thanked. Mr. Björn Palmberg is appreciated for offering helpful comments.

References

[1] Szolwinski MP, Farris TN. Mechanics of fretting fatigue crack formation. Wear 1996;198:93–107.

[2] Finney JM, Evans RL. Extending the fatigue life of multi-layer metal joints. Fatigue and Fracture of Engineering Materials and Structures 1995;18(11):1231-1247.

[3] Segerfröjd G. Fractographic observation of initiation sites and early growth in mechanical joints. Doctoral thesis 99-28. Department of Aeronautics, Royal Institute of Technology, Stockholm, Sweden, 1999.

[4] Terada H. Structural fatigue and joint degradation. International Journal of Fatigue 2001;23:21-30.

[5] Atzori P, Lazzarint P, Quaresimin M. A re-analysis on fatigue data of aluminium alloy bolted joints. International Journal of Fatigue 1997;19(7):579-588.

[6] Shankar K, Dhamari R. Fatigue behaviour of aluminium alloy 7075 bolted joints treated with oily film corrosion compounds. Materials and Design 2002;23:209-216.

[7] Ireman T. Three-dimensional stress analysis of bolted single-lap composite joints. Composite Structures 1998;43(3):195-216.

[8] Moretti LR, Segerfröjd G, Palmberg B. Fatigue behaviour of mechanical joints: a programme overview and an introduction to fretting and fretting fatigue with special application to joints. Report FFA TN 1998-03, Swedish Defence Research Agency, 1998.

[9] Palmberg B. Instrumented bolts for measurements of their shear load transfer in single and double shear joints. Report FFA TN 1991-09, Swedish Defence Research Agency, 1991.

[10] Moretti LR, Palmberg B, Segerfröjd G. Fatigue testing of medium and high load transfer joints. Report FFA TN 1998-30, Swedish Defence Research Agency, 1998.

[11] Melin GL. Optical whole field measurement techniques for mechanical testing – a review. Report FFA TN 1999-35, Swedish Defence Research Agency, 1999.

[12] Ekh J. Multi fastener, composite-to-aluminium, single-lap joints. Presentation on the BOJCAS progress meeting, Royal Institute of Technology, Stockholm, Sweden, 2001.

[13] Young RD, Rose CA, Starnes JH. Skin, stringer, and fastener loads in buckled fuselage panels. Presented at the 42nd AIAA/ASME/ASCE/AHS/ASC Structures, Structural Dynamics, and Materials Conference, Seattle, Washington, AIAA 2001-1326, April 16-19, 2001; pp. 1-18.

[14] Friberg G. Fastener load distribution and interlaminar stresses in composite laminates. Licentiate thesis 2000-18. Department of Aeronautics, Royal Institute of Technology, Stockholm, Sweden, 2000.

[15] Eriksson P, Magnusson A. Determination of load transfer distribution of bolted shear joint by integration method. Report FFA HU-2332/1, Swedish Defence Research Agency, 1982.

[16] Starikov R. Quasi-static and fatigue behaviour of composite bolted joints. Doctoral thesis 2001-9. Department of Aeronautics, Royal Institute of Technology, Stockholm, Sweden, 2001.

[17] Gustafsson B, Sjöberg A, Abrahamsson L. Numerisk lösning av differentialekvationer. Department of Scientific Computing, Uppsala University, Sweden, February 1988. *In Swedish.*